Title	THE CRYSTAL STRUCTURES OF FERROELECTRIC NH_4H(ClCH_2COO)_2 AND ITS RELATIONSHIP ON THE ISOTOPE EFFECT OF THE HYDROGEN BOND
Author(s)	Ichikawa, Mizuhiko
Citation	大阪大学, 1979, 博士論文
Version Type	VoR
URL	https://hdl.handle.net/11094/24572
rights	
Note	

The Crystal Structures of Ferroelectric $NH_4H(ClCH_2COO)_2$
and Its Relationship on the Isotope Effect
of the Hydrogen Bond

A Thesis
Submitted to the Faculty of the Graduate School of
Osaka University

By
Mizuhiko Ichikawa

In Partial Fulfilment of the Requirements
for the Degree of
Doctor of Philosophy

Synopsis

The Crystal Structures of Ferroelectric $NH_4H(ClCH_2COO)_2$ and

Its Relationship on the Isotope Effect of the Hydrogen Bond

A brief historical description of ferroelectrics and
ferroelectric phenomena is given. In this context, a
particular significance of the structural studies in
ferroelectric $NH_4H(ClCH_2COO)_2$ with a possibility of a
single-minimum potential well of the acidic H atom is
emphasized. Furthermore, the significance of studying the
characteristic of the hydrogen bond and the isotope effect
from the viewpoint of the bonding parameters is described.

In chapter II the results of the structure analysis
in the paraelectric phase at room temperature are described,
in which the final R value was 0.068. It is found that
$NH_4H(ClCH_2COO)_2$ has the shortest symmetric hydrogen bond,
2.432(5) $\overset{\circ}{A}$, connecting two chloroacetate residues among
hydrogen-bonded ferroelectrics. It is concluded that
the shape of the hydrogen-atom potential is effectively
of a single-minimum type and $NH_4H(ClCH_2COO)_2$ is the first
example with a single-minimum potential well, from the
O...O length and the anomalous characteristic of the infrared
spectrum together with the conclusion drawn from the neutron
diffraction and spectroscopic data in other Type A acid
salts.

In chapter III the results of the structure analysis
in the ferroelectric phase at 80 K is given, in which the
final R value was 0.106. No appreciable change was
found in the conformation of the chloroacetate dimers
including the very short hydrogen bond (2.457 $\overset{o}{A}$), whereas
a considerable shift in the ammonium ion was observered.
The mechanism of ferroelectric phase transition is discussed.
The order-disorder model of the acidic hydrogen atom is
excluded since the hydrogen atom in a single-minimum
potential cannot play the crucial role in the phase
transition, in contrast to the order-disorder model adopted
usually in hydrogen-bonded ferroelectrics with assumption
of a double-minimum potential well such as in KH_2PO_4. The
conclusion is compatible with that from other experimental
technique mainly by Chihara and coworkers, i.e. the ^{35}Cl nuclear
quadrupole resonance frequency and relaxation time, the
heat capacity measurement, and infrared and Raman spectra.
A possibility of a pure order-disorder mechanism of the
nitrogen atom in the ammonium ion was examined, but was
ruled out from the consideration of the shape of Fourier
map and the r.m.s amplitude of thermal vibrations. This
conclusion is also compatible with other experiments.

Chapter IV is related to the correlation between O-H vs
O...O distances and the geometric isotope effect ΔR in OHO
bonds. Symmetric bonds are continuously distributed at
least up to about 2.6 $\overset{o}{A}$, in which the shape of the H atom

potential curve seems to vary continuously from single to double-minimum type with increasing O...O distance, retaining the symmetry requirement. The average correlation curve of asymmetric bonds appears to coincide with 'symmetric' straight line at the shortest limit around 2.4 $\overset{\circ}{A}$. On deuteration an expansion was seen in the O...O distance range 2.44-2.64 $\overset{\circ}{A}$.

The equilibrium position of the H atom in symmetric bonds is considered with two correlation curves (O-H vs O...O and ΔR vs O...O) used as empirical basis, under assumption that the potential curve can be expressed as the superposition of two asymmetric bonds. The correspondence is pointed out between two kinds of the isotope effect, i.e. the isotope effect of the distance between two equilibrium positions (or ΔR) and the isotope effect of the transition temperature in hydrogen-bonded crystals which undergo ferro-, antiferroelectric, and other structural phase transitions.

Contents

Contents   (continued)

Chapter I. Introduction

I.1. Ferroelectricity and hydrogen bond

The first ferroelectric, Rochelle salt, was discovered in 1920 and the second, KH_2PO_4 (KDP), in 1935. These two crystals were the only two known ferroelectrics before the discovery of $BaTiO_3$ after World War II. Thus, the hydrogen bond was in intimate relations with ferroelectricity from the times that ferroelectricity appeared to be a rare and isolated phenomenon and was considered to be 'one of Nature's great accidents' (B. T. Matthias). It was plausible that not only OHO but NHO hydrogen bond may be important for the occurrence of ferroelectricity and was a clue to searching new ferroelectrics, in the course of the subsequent discoveries of $(NH_2)_3Al(SO_4)_2 \cdot 6H_2O$ (GASH), $(NH_2CH_2COOH)_3 \cdot H_2SO_4$ (TGS), a number of alums, and $(NH_4)_2SO_4$ and so on. (See, for example, Jona and Shirance,[1] and Landolt-Bernstein[2])

Recently the number of known ferroelectrics amounts to a few hundreds, a considerable part of which are yet the hydrogen-bonded ferroelectrics, with various types of the hydrogen bond such as OHO, NHO, ClHCl. Today ferroelectricity is no more isolated phenomenon, but occupies a definite position as a field in the solid state

physics and chemistry.

It should be borne in mind here that among many hydrogen-bonded ferroelectrics,

(i) there are a great variety of the hydrogen-bond strength, i.e. the hydrogen-bond length (the distance between a donor and an acceptor atom), and several types of the hydrogen-bond such as OHO, NHO, ClHCl.

I.2. Developement of studies of displacive-type ferroelectrics by the soft-mode concept

The discovery of the third ferroelectric $BaTiO_3$ in 1945-46 was a great step in advance toward a better understanding of ferroelectric phenomeon; its structure is far simpler than that of any other ferroelectric known and is common to large family of compounds called perovskite-type structure. It was shown by Devonshire[3] that three successive phase transitions in $BaTiO_3$ can be described phenomenologically by taking the cubic perovskite structure as prototype. In 1960 it was proposed by Cochran[4] and also by Anderson[5] that the phase transition for the $BaTiO_3$-type ferroelectrics results from an instability of one of the normal vibrational modes of lattice (soft-mode theory). In this theory, the phonon frequency of a particular transverse optic mode ω_{TO} decreases and tends to zero on approaching the transition temperature T_c with

$$\omega_{TO}^2 = A(T - T_o) \quad ,$$

where A is a constant, T_o the paraelectric Curie temperature. At T_c the restoring force for the mode displacement become zero and this soft phonon motion freezes into the static displacement of the low-temperature phase.

The neutron scattering occupies a unique position as a very powerful tool among many experimental technique; it has important advantages in contrast to light and X-ray scattering because the neutron scattering can cover a wide range of Q and the neutron energy $\hbar\omega$ is of the same order of magnitude with phonon in measuring the scattering function $S(Q, \omega)$ by which the dynamical properties of solids can be characterized.[6] Experimental development of the neutron inelastic scattering revealed the soft mode condensation of Γ (q = 0) mode at Brillouin zone center in the displacive-type ferroelectrics with perovskite structure such as $BaTiO_3$, $PbTiO_3$, $KNbO_3$, and $KTaO_3$. Furthermore the inelastic neutron scattering made possible the mode determination from intensity analysis, i.e. to obtain the atomic motion involved in the soft mode, in $KTaO_3$ and several other cases.[7]

Apart from the perovskite-type displacive ferroelectrics, the soft mode concepts was extended to order-disorder type[8] and to zone boundary phonon[9]; The soft mode condensations at Γ point in order-disorder ferroelectric KD_2PO_4, at M point of Brillouin zone boundary in ND_4Br,

at M point in ferroelectric $Tb_2(MoO_4)_3$, at M and R points in perovskite $SrTiO_3$, $KMnF_3$, $NaNbO_3$, $LaAlO_3$ are examples.[7] The soft phonons are also observed in other various structural phase transitions; their examples are the Γ mode condensation in quartz, in semiconductor GeTe, SnTe etc., and the transverse acoustic (TA) mode softening in superconductor Nb_3Sn, V_3Si.[7] Recently the structural phase transitions in some MX_2-type 2-dimensional metals and in 1-dimensional conductors KCP and TTF-TCNQ are discussed in terms of enhanced Kohn anomaly (acoustic phonon softening at $q = 2 k_F$) through electron-phonon interaction. Studies along these lines are now in progress and present interesting topics such as 'central modes problem'.[10,28]

Thus, the generalization of the soft mode concept brought the unified understanding of the fundamental mechanism of structural phase transitions. It can be said again that ferroelectricity is no more isolated phenomenon, but has many related phenomena and common mechanisms with other field of solid state physics and chemistry, in addition to the well known similarity and dissimilarity to ferromagnetism.

I.3. Anomalously large isotope effects on physical quantities in some hydrogen-bonded ferroelectrics.

In order to understand better the nature of

ferroelectricity on the basis of knowledge obtained from the lattice dynamical approach such as the soft-mode concept, knowledge of structural details and chemical-bonding characteristic in individual ferroelectric crystal is necessary; Both approaches may be said to be the complement of each other. Importance of static 'structural' approaches should be emphasized because ferroelectrics have generally complex structure with relatively low symmetry and with many atoms in an asymmetric unit. One of the clues to the unified understanding from the structural point of view may be the hydrogen bonding, as can be seen from (i).

The most striking and dramatic phenomenon in hydrogen= bonded ferroelectrics is anomalous isotope effects on some physical properties such as transition temperature T_c which are seen in some acid salt crystals such as KH_2PO_4 (KDP) type crystals. Transition temperature rises about 100 K by substituting deuterium for hydrogen atom $(H \rightarrow D)$[11]; This isotope effect is very remarkable and not so much precendented over the fields in solid state physics. It seems to be owing to these circumstances that the hydrogen-bonded ferroelectrics mean KDP-type ferroelectrics in a narrow sense.

The first molecular theory of the phase transition in KH_2PO_4 was proposed by Slater in 1941,[12] where he assumed prior to experimental evidence that each proton, which is contained in the OHO bond linking neighbouring PO_4 groups, takes one of two positions in a double-minimum potential well

(order-disorder model). After about a decade, Bacon and Pease[13] showed by neutron-diffraction structure analysis that an average density distribution of proton changes remarkably through the transition temperature; this result was <u>compatible</u> with Slater's assumption. Furthermore, in order to explain the large isotope effect, Blinc[11] and subsequently Tokunaga and Matsubara[14, 15] proposed a proton tunneling model in which proton is assumed to make a tunneling motion between two minima of the double-minimum potential well. Subsequently Kobayashi[15] took into consideration the coupling between transverse optic mode in $K-PO_4$ ion and the tunneling motion of proton (spin-phonon coupling).[17] Thereafter very extensive experimental and theoretical work has been reported. However, the problem of the origin of anomalously large isotope effect is still one of the main problems in the fields of ferroelectricity today, but does not attain to the complete understanding.[18, 19]

Assumptions used in the theories of phase transition of KH_2PO_4, i.e. that the proton is distributed in a double-minimum potential and that proton play a crucial role (trigger) in phase transition, seem to exert farreaching influence on the phase-transition mechanism of the other general hydrogen-bonded ferroelectrics explicitly or implicitly. For example, the same phase transition mechanism as KDP was proposed in TGS by Hoshino, Okaya and Pepinsky.[20] However, recently Fletcher, Keve and Skapski state that it is difficult to accept any major role attributed

to proton in the short hydrogen bond connecting two glycine molecules as the motive force for the phase transition.[21] It should be stressed here again that next points are assumed in the KH_2PO_4 theories;

    (ii) the potential shape is of a double-minimum type,

    (iii) the hydrogen-bond length O...O or the potential

    shape of the proton does not change by $H \rightarrow D$.

B. T. Matthias states in the paper[22] with the title of "Ferroelectricity: Why did it take so long?" that "Very often in science a mistaken notion expressed by one or a few investigators has had a very decisive influence for an inordiately long time afterwards both on the correct and incorrect work of a great many hundred believers. Again and again this has happended".

I.4. A peculiar significance of ferroelectrics with the potential curve of single-minimum type

The shape of the potential curve may probably be of single-minimum type in the very short hydrogen bond, where the hydrogen atom cannot be a trigger of the phase transition. Thus, it may be possible that the role of the phase transition differs in each compound; some may play the crucial role (a trigger), but some play only the secondary role, since the hydrogen bond, involved in many hydrogen-bonded ferroelectrics, are full of variety.

The potential of hydrogen atom of a single-minimum type is supposed to be realized in the FHF hydrogen bond (See, for example, Hamilton and Ibers[23]). With reference to the OHO system, a group of acid salts of carboxyl acids, classified as Type A and A_2, attracts particluar attention.[24] Firstly, Type A and A_2 acid salts involve most of the shortest OHO bonds so far measured, whose O...O length are concentrated with a mean of 2.445(2)Å and 2.450(2)Å respectively. Secondly, the conclusion with respect to the potential shape, obtained from neutron diffraction and spectroscopic techniques, is converged into the opinion that

(iv) in all type A acid salts, the hydrogen bond has the potential curve of effectively single-minimum type.

Furthermore, it has been found by us[25] that

(v) ammonium hydrogen bis-chloroacetate, $NH_4H(ClCH_2COO)_2$, is a member of Type A acid salts and exhibits ferroelectricity.

These results strongly suggest the possibility that $NH_4H(ClCH_2COO)_2$ has also a very short hydrogen bond as in all other members of Type A acid salts, and this compound offers the first example of ferroelectrics with a single-minimum potential, where the hydrogen bond is too short to play the role as trigger of the phase transition. Thus, the experimental verification of the hydrogen-bond structure by the crystal structure analysis of $NH_4H(ClCH_2COO)_2$ seems indispensable for further and more general understanding of the phase-transition mechanism in

hydrogen-bonded ferroelectrics.

I.5. Correlations between hydrogen-bond parameters and
geometric isotope effect in OHO hydrogen bonds

From now discussion is restricted within the OHO bond
because much data are available, there are full of variety
in the OHO bond, and present interest is concentrated on the
short and very short bond. It is commonly said that, as
illustrated in Fig.1 the potential function for a hydrogen
atom in a hydrogen bond may be characterized qualitatively
by one of the curves, which may perhaps be determined by the
factors as the O...O distance, symmetry and surroundings of
the hydrogen bond. Hydrogen-bond parameter, such as O-H,
H...O, O...O length and OHO angle, can be obtained by
X-ray and neutron-diffraction structure analyses. But X-ray
data are inadequate because of inaccuracy of the hydrogen-atom
position. The existence of correlation between O-H and
O...O length was first pointed out by Nakamoto, Margoshes
and Rundle[26] in 1955; the O-H decreases with increasing
the O...O distance. Since then correlations between
hydrogen-bond parameters has been refined according to the
accumulation of data at that time, and seems well
established in an intermediate and long region of O...O
distance. However,

(vi) for the short and very short region, about
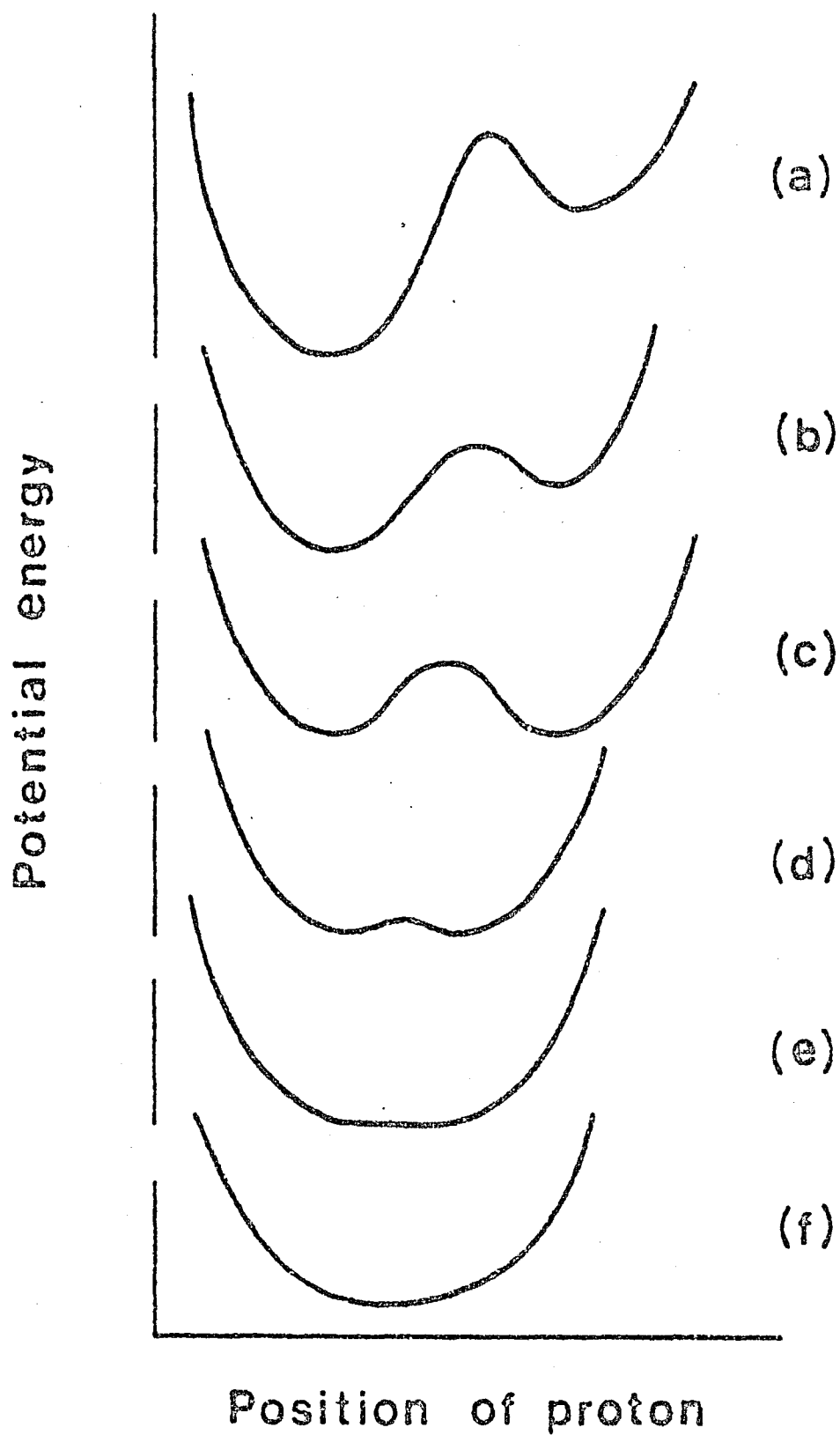
Fig. 1.   Schematic illustration of possible potential energy curves for OHO bonds, assumed to be characteristic of different O...O length.

O...O $<$ 2.6 Å, the correlation remain unsettled with

respect to the dependence on the O...O distance and

symmetry of the hydrogen bond.

This may probably be partly because the compounds having

the short and very short hydrogen bond are rare, partly

because both of the facilities and precision of neutron

diffraction structure analyses were insufficient yet for

present purpose.

The other key problem from structural aspects is a

geometrical isotope effect, i.e. the variation of the O...O

distance when deuterium is substituted for hydrogen. From

about four decades before, it has been pointed out by

Ubbelohde and co-workers[27] that an expansion of the O...O

distance is observed. However,

(vii) there is uncertainty about whether the size of the

geometric isotope effect exhibits the O...O dependence

and how large is it.

This circumstances seem to arise from that magnitude of the

effect is usualy as small as $\sim 10^{-2}$Å and thus an accuracy

of $\sim 10^{-3}$Å are required in both of the hydrogen and the

deuterium compounds.

I.6. Scope of this paper

Generally speaking, what role the hydrogen bond plays

in the phase transition of hydrogen-bonded ferroelectrics

and other related materials? Where anomalously large

isotope effects results from?

In order to elucidate these problems, as emerge from

(i) $\sim$ (vii) described above, first of all the next points

may be indispensable:

(1) to verify experimentally an example of ferroelectrics

with the hydrogen-atom potential of a single-minimum

type, i.e. the crystal structure analysis of ferroelectric

$NH_4H(ClCH_2COO)_2$ at present.

(2) to establish the characteristic of the potential

shape of the hydrogen atom under the condition of a

definite O...O distance, symmetry of the hydrogen bond,

together with the information from spectroscopic

measurements.

(3) to build up the details of the geometric isotope

effect on the O...O distance and other factors dependence.

(4) to consider the phase-transition mechanism for

the explanation of observed physical quantities on the

basis of the latest information of the hydrogen-bond

structure, such as, from (2) and (3).

(5) to find out the condition and origin of the anomalous

isotope effect.

Studies of this paper have been performed under the

strategy described above.

References

1) F. Jona and G. Shirance: Ferroelctric Crystals
   (The Macmillan Company, New York, 1962).

2) T. Mitsui: Landolt-Börnstein. Numerical Data and
   Functional Relationships in Science and Technology
   ed. K. -H. Hellwege and A. M. Hellwege (Springer,
   Berlin, 1969) New Series III/3. Ferro- and
   Antiferroelectric Substances.

3) A. F. Devonshire: Phil. Mag. $\underline{40}$ (1949) 1040; Advances
   in Phys. $\underline{3}$ (1954) 85.

4) W. Cochran: Advances in Phys. $\underline{9}$ (1960) 387.

5) P. W. Anderson: Fizika dielekrikov, ed. G. I. Skanavi
   (Acad. Nauk SSSR, Moscow, 1960) 290.

6) W. Cochran: The Structures and Properties of Solids 3
   The Dynamics of Atoms in Crystals (Edward Arnold,
   London, 1973) Chap.5.

7) G. Shirane: Rev. mod. Phys. $\underline{46}$ (1974) 437.

8) W. Cochran: Advances in Phys. $\underline{10}$ (1961) 401.

9) W. Cochran and A. Zia: Phys. Status Solidi
   $\underline{25}$ (1968) 273.

10) Anharmonic Lattices, Structural Transitions and Melting,
    ed. T. Riste (Noordhoff, Leiden, 1974).

11) R. Blinc: J. Phys. Chem. Solids $\underline{13}$ (1960) 204.

12) J. C. Slater: J. Chem. Phys. $\underline{9}$ (1941) 16.

13) G. E. Bacon and R. S. Pease: Proc. Roy. Soc.
    $\underline{A220}$ (1953) 397; $\underline{A230}$ (1955) 359.

14) M. Tokunaga and T. Matsubara: Progr. Theor. Phys. 35 (1966) 581.

15) M. Tokunaga: Progr. Theor. Phys. 36 (1966) 857.

16) K.K. Kobayashi: J. Phys. Soc. Japan 24 (1968) 497.

17) W. Cochran: Advances in Phys. 18 (1969) 157.

18) M. Tokunaga: Ferroelectrics 1 (1970) 195.

19) G. A. Samara: Ferroelectrics 5 (1973) 25.

20) S. Hoshino, Y. Okaya and R. Pepinsky: Phys. Rev. 115 (1959) 323.

21) S. R. Fletcher, E. T. Keve and A. C. Skapski: Ferroelectrics 14 (1976) 775; 14 (1976) 789.

22) B. T. Matthias: Ferroelectrics 16 (1977) 21.

23) W. C. Hamilton and J. A. Ibers: Hydrogen Bonding in Solids (Benjamin, New York, 1968) Chap.3.

24) J. C. Speakman: Structure and Bonding 12 (1972) 141.

25) M. Ichikawa and T. Mitsui: Phys. Rev. 152 (1966) 495.

26) K. Nakamoto, M.Margoshes and R. E. Rundle: J. Amer. Chem. Soc. 77 (1955) 6480.

27) J. M. Robertson and A. R. Ubbelohde: Proc. Roy. Soc. London. A170 (1939) 222; A. R. Ubbelohde: Proc. Roy. Soc. London. A173 (1939) 417; A. R. Ubbelohde and I. Woodward: Proc. Roy. Soc. London. A179 (1942) 399.

28) R. Blinc and B. Zeks: Soft Modes in Ferroelectrics and Antiferroelectrics (North-Holland, Amsterdam, 1974)

Chapter II. The X-ray Crystal Structure Analysis of

   Ferroelectric $NH_4H(ClCH_2COO)_2$ of the Paraelectric

   Phase at Room Temperature ,

II.1. Introduction

   It has been discovered that ammonium hydrogen

bis (chloroacetate) $NH_4H(ClCH_2COO)_2$, is ferroelectric

below 128 K.[1] This compound belongs to acid salts MHX_2

of monocarboxylic acid HX. It is known that a group of

MHX_2 compounds called Type A involve the very short

hydrogen bond connecting two X with the hydrogen-atom

potential of single-minimum type.[2] Ferroelectric

$NH_4H(ClCH_2COO)_2$ is of a particular interest in connection

with the phase-transition mechanism and the hydrogen-atom

potential function in OHO bond, since ordinarily the

phase-transition mechanism of hydrogen-bonded ferroelectrics

with short hydrogen bonds are interpreted in terms of

order-disorder model, where the hydrogen positions are

assumed to be distributed between double minima in the

potential functions.

   With a special attention to the hydrogen-bond

structure, a three dimensional X-ray crystal structure

analysis of the paraelectric phase has been carried out

at room temperature.[3]

II.2. Experimental

Crystal data

The crystal data of ammonium hydrogen bis (chloroacetate) are given in Table 1, of which preliminary results were previously reported.[1] Unit-cell parameters at room temperature were obtained from a least-squares treatment, using values of θ for 74 high angle reflections measured on zero-layer Weissenberg photographs taken around each crystallographic axis with CuKα radiation. In this procedure, the systematic errors due to inaccurate value of Weissenberg camera radius and due to shrinkage of X-ray films are corrected using Al as standard material. Systematic errors from deviation of specimen from the center of the camera and due to other causes were taken into consideration by adding a term proportional to $\sin2\theta$ in the observation equations.

Data collection

Two sets of three-dimensional intensity data were used in this work; one is phtographic data and other is diffractometer data. The first set was obtained from equi-inclination Weissenberg photographs taken with CuKα radiation using the multiple film technique about a, b, and c axes. Following efforts were directed to obtain accurate data. Integrated Weissenberg photographs with seven films were taken with exposure of 60 KV, 100 mA, and

Table 1.   Crystal data

$$a = 10.521.(4) \ \overset{\circ}{A}$$
$$b = 11.576 \ (4)$$
$$\underline{c} = 8.387 \ (3)$$
$$\beta = 119.48 \ (3) \ ^{\circ}$$
$$\underline{V} = 889.2 \ (5) \ \overset{\circ}{A}{}^3$$

Formula : $NH_4H(ClCH_2COO)_2$

Space group $C2/c$

F. W.   206.0

$\rho_m = 1.528$ $g.cm^{-3}$

$\rho_c = 1.538$ $g.cm^{-3}$

$F(000) = 424$

$\underline{Z} = 4$

$\lambda(Cu \ K\alpha_1) = 1.5405 \ \overset{\circ}{A}$

about half a day. As many photographs as possible were
taken to get the reliable scaling factors and many
number of reflections, as far as the camera setting is
permitted, i.e. layer: h = 0~6; k = 0~7; l = 0~5.
Cylindrical crystals with dimension of 0.22~0.24 mm in
diameter were used. The intensities were measure by visual
comparison with a calibrated scale. They were corrected
for Lorentz and polarization factors, absorption correction
being applied (μCuKα = 63 cm^{-1}). Absorption correction
factors used for calculation were taken from International
Tables for X-ray Crystallography. [4]   Corrections for
the elongation of spots on the high layers were made
according to Phillips.[5] The data from each layer were
correlated by the method of Rollett and Sparks[6] and then
placed on an absolute scale by Wilson's method.[7]
A total of 738 independent reflections were obtained,
of which 227 were too weak to be measured.

The second set of data were obtained on a Rigaku
Denki automatic four-circle diffractometer, AFC,
controlled by a FACOM 270-20 computer. A spherical
crystal with dimension of 0.35 mm in diameter was used.
Integrated intensities were collected for $2\theta \leq 70°$ by
the $\omega - 2\theta$ scanning technique with Mo Kα radiation
monochromatized with a LiF crystal. A scanning speed of
2° per minute was employed and the scanning range varied
by $\Delta 2\theta = 2° + 0.8°\tan\theta$. Background was measured for
twenty seconds at the beginning and at the end of each scan.

As a check on the stability of the crystal and the
instruments, three standard reflections were measured
every fifty reflections: no singificant variation in
their intensities was noted. No correction was made for
absorption (μMoKα = 7.0 cm^{-1}). A total of 1967
reflections were measured, of which 706 had the $\left|F_o\right|$ values
less than three times its standard deviation derived from
counting statistics, and were given the value of zero.
The calculation of the unit-cell parameters and the whole
processing of intensity data were carried out on a
HITAC 5020E computer with UNICS.[8]

II.3. Determination and refinement of the structure

Phase determination

As is well known, electron-density distribution
ρ(x,y,z) is expressed by

$$\rho(x,y,z) = \frac{1}{V} \sum_h \sum_k \sum_l F(hkl)\exp[-2\pi i(hx + ky + lz)]$$

, where V is unit-cell volume, (hkl) indicates Miller
indices. However, we can not obtain directly the
structure factor F(hkl), since F(hkl) is usualy complex
and only the magnitude $\left|F(hkl)\right|$ is known from intensity
measurements;

$$F(hkl) = \left| F(hkl) \right| \exp[i\alpha(hkl)] \quad .$$

Thus it becomes nesessary to know the phases $\alpha(hkl)$; This is called 'phase problem' and is essentially one of the key problems for structure determination. This problem is now developing.

One of the important situations in which the phases can be determined is that the compound involves a heavy atom, whose scattering power dominates, and controls some or all phases. Then the structure factor is written by

$$F(khl)$$
$$= \sum_{H=1}^{Z} f_H \exp[2\pi i(hx_H + ky_H + lz_H)] + \sum_{j=1}^{N-Z} f_j \exp[2\pi i(hx_j + ky_j + lz_j)] \quad ,$$

where Z and N denote the number of heavy atoms and total atoms in unit cell respectively, f_H and f_j are atomic scattering factors of heavy atom and other light atoms respectively, (x_H, y_H, z_H) and (x_j, y_j, z_j) are the position of heavy atoms and other light atoms respectively. The first term on the right hand side expresses the contribution of heavy atoms and the second is that of other light atoms. On the other hand the phase $\alpha(hkl)$ is given by

$$\alpha(hkl)$$
$$= \tan^{-1} \frac{\sum f_H \sin 2\pi(hx_H + ky_H + lz_H) + \sum f_j \sin 2\pi(hx_j + ky_j + lz_j)}{\sum f_H \cos 2\pi(hx_H + ky_H + lz_H) + \sum f_j \cos 2\pi(hx_j + ky_j + lz_j)} \quad .$$

If the light atoms are distributed in relatively uniform fashion, it will be expected that the second terms in a numerator and a denominator cancel each other. Then the phase $\alpha(hkl)$ will be approximately equal to the phase $\alpha_H(hkl)$ from heavy atoms only:

$$\alpha(hkl) \simeq \alpha_H(hkl) \quad .$$

Thus the phases can be obtained if we know the heavy-atom position. Fourier synthesis with the heavy-atom phases reveals the positions of other atoms and ordinarily several Fourier syntheses with the phases refined successively lead to satisfactory results. This method for the phase determination is called 'heavy atom method'.[9] It is roughly said that the heavy atom method is good approximation when

$$\sum f_H^2 \sim \sum f_j{}^2$$

holds.

One way of locating of the heavy atom is with the aid of Patterson synthesis. The Patterson function is defined as

$$P(u,v,w) = \int_0^1 \int_0^1 \int_0^1 \mathcal{S}(x,y,z)\mathcal{S}(x+u,y+v,z+w)Vdxdydz$$

and can be represented by Fourier series

$$P(u,v,w) = \frac{1}{V}\sum_h \sum_k \sum_l \left| F(hkl) \right|^2 \exp[-2\pi i(hu+kv+lw)] \quad .$$

Patterson function is an auto-correlation function of electron density, which is obtainable directly from experiment, and gives the vector distance between every pair of atoms in a unit cell. Thus, the peaks showing the distance between heavy atoms is far and away high among the peaks of other various pair of atoms, from which the heavy-atom position is obtained.

Refinement procedure

The phase determination and successive Fourier syntheses for structure determination were performed along the line described above; for $NH_4H(ClCH_2COO)_2$ has the heavy atom Cl, which satisfies the suitable condition for heavy atom method. The structure determination was initiated using the photographic data. The coordinates of the chlorine atoms were determined from a three-dimensional sharpened Patterson function. Four cycles of Fourier iterations led to an R value ($\sum |k|F_o| - |F_c||/ \sum k|F_o|$) of 0.26. Refinement was carried out using a block-diagonal least-squares method for positional parameters, and individual isotropic and anisotropic temperature factors. The quantity minimized was $\sum w(|F_o| - 1/k|F_c|)^2$. A difference Fourier syntheses revealed all the hydrogen atoms at the expected positions.

At this stage the diffractometer data became available and subsequent least-squares calculations were performed with these data. The starting parameters were

those obtained in the final cycle of the isotropic

refinement using photographic data. Refinement was carried

out on the coordinates of heavy atoms with anisotropic

temperature factors and on the coordinates of hydrogen

atoms with isotropic temperature factors. The temperature

factor of H(3) atom, however, was given a fixed value of the

overall temperature factor, because its value was found to

be unusually large. All parameter shifts were less than

one tenth of their standard deviations in the final cycle.

The standard deviations of the parameters were calculated

from the sum of the weighted residuals and the diagonal

terms of the inverse matrix of the normal equations.

Unit weight was assigned for all the reflections, except

those with zero intensity and five strong refletions which

are likely affected by extinction; these five reflections

were given zero weight in the refinement. The damping

factor of 0.8 was applied to the scale factor, the overall

temperature factor and also to the parameters of the

heavy atoms, and 0.1 to those of the hydrogen atoms.

The final R value for the counter data was 0.068 (0.070

for photographic data). Atomic scattering factors were

taken from International Tables for X-ray Crystallography.[4]

Fourier, least-squares, bond-length and bond-angle,

and best-plane calculations were done on a HITAC 5020E and

a FACOM 230-60 computer with UNICS.[5] The final positional

parameters and temperature factors are given in Tables 2 and

3 respectively, together with their standard deviations

Table 2.   The atomic positional parameters and their
standard deviations (e.s.d.'s in Å)

	x	y	z	σ(x)	σ(y)	σ(z)
Cl	0.1842	0.4237	-0.0607	0.0011	0.0011	0.0010
O(1)	0.1770	0.2548	0.3340	0.0025	0.0023	0.0025
O(2)	0.3401	0.3781	0.3363	0.0021	0.0019	0.0021
N	0.0000	0.0453	0.2500	_____	0.0032	_____
C(1)	0.1161	0.3404	0.0575	0.0034	0.0034	0.0037
C(2)	0.2242	0.3255	0.2580	0.0028	0.0025	0.0032
H(1)	0.2500	0.2500	0.5000	_____	_____	_____
H(2)	0.0727	-0.0045	0.2366	0.0386	0.0362	0.0392
H(3)	0.0351	0.0820	0.3521	0.0418	0.0349	0.0361
H(4)	0.0906	0.2678	-0.0055	0.0391	0.0353	0.0376
H(5)	0.0283	0.3785	0.0479	0.0447	0.0366	0.0417

Table 3.   The temperature factors and their standard deviations ($\times 10^4$).

The anisotropic temperature factors are of the form :

$$\exp\left\{-(\ \beta_{11}h^2 + \beta_{22}k^2 + \beta_{33}l^2 + \beta_{12}hk + \beta_{13}hl + \beta_{23}kl)\right\}.$$ The temperature factors for hydrogen atoms are isotropic B ($\overset{\circ}{A}{}^2$).

	β_{11}	σ	β_{22}	σ	β_{33}	σ	β_{12}	σ	β_{13}	σ	β_{23}	σ
Cl	144	1	127	1	207	2	−69	2	76	2	98	2
O(1)	140	3	96	2	243	5	−107	4	182	6	8	5
O(2)	92	2	69	2	193	4	−48	3	121	5	−4	4
N	80	3	55	2	291	9	0	−	126	9	0	−
C(1)	106	3	92	3	232	7	−61	5	84	8	30	7
C(2)	89	3	54	2	208	5	−21	4	133	7	−16	5
H(1)	8.1	(1.9)										
H(2)	3.7	(0.8)										
H(3)	4.1	(−)										
H(4)	3.6	(0.8)										
H(5)	4.7	(0.9)										

and list of $|F_o|$ and F_c values for the counter data is given in Table 4 (for photographic data in Table 5). In Fig.1 a composite drawing of a three-dimensional electron-density map is shown, while in Fig.2 that of a difference map is shown, for which the contributions of the hydrogen atoms were excluded from the calculated structure factors.

II.4. Description of the structure

Type-A acid salts

The structure viewed along a and b axes is shown in Figs.3 and 4, respectively. A layer of ammonium ions, lying in the (40$\bar{4}$)-planes, has a layer of chloroacetate residues on either side, or vice versa, and the packing between the ammonium ion and the chloroacetate residue is dominated by a three-dimensional network of hydrogen bond. Moreover, two chloroacetate residues are related to one another by a symmetry center, across which they are linked by a hydrogen bond involving the acidic hydrogen atom. According to Shrivastava and Speakman, these structural features of ammonium hydrogen bis (chloroacetate) are the characteristic of acid salts, MHX_2, of monocarboxylic acid, HX, belonging to Type A. In Type B two acidic radicals are crystallographically distinct. Type-A acid salts found so far are summarized in Table 6.

Table 4. Observed and calculated structure factors (× 10) for the counter data.

Table 4.   (continued)

```
  K  FO  FC      K  FO  FC      K  FO  FC      K  FO  FC      K  FO  FC      K  FO  FC      K  FO  FC      K  FO  FC      K  FO  FC      K  FO  FC

H,L= -6   7     15  31 -21     10  26  16      4  61 -72      2  77  83    H,L=  6    8      5  49  56      4  25  26      7  45  42     10  32 -31
   2 146 131    H,L=  0    7   H,L=  7    7      6 113-111      4 122-118      0  39 -37      7  56  57    H,L=  5    9     19  35  47    H,L= -5  11
   4  43  34      4  55 -54      3  47  48     10  29  19      6  92 -92      6  30  21     13  26 -24      1  29  -9    H,L= -2  10      3  45 -38
   6  67 -69      6  90 -96      5  27  33    H,L= -7   8     10  37  41    H,L=-13   9    H,L= -4   9    H,L=-14  10      0  60  76      7  38  30
   8  91 -83      8  26 -13      7  24 -74      1  48  55     14  26   6      1  31  12      2 111-105    H,L=-13  10      6  60 -56    H,L= -4  11
  10  36  35     10  64  76    H,L=-16   8      3  43 -36    H,L= -1   8      7  54 -48      4 114-119     10  31   4      4  37 -26
  12  48  36     14  24  -5      2  74   6      5  86  87      1 112 112    H,L=-12   9      8  40  47    H,L= -1  10      6  39 -35
H,L= -5   7    H,L=  1    7    H,L=-14   8      9  55 -54      3  24  26      4  33  31    H,L= -3   9      1  28 -21     10  31  25
   1 212 196      1 132 135      0  77  78     11  27 -28      5  51 -40      8  33 -33      5  27  26      5  57  49    H,L= -3  11
   3 245 244      3 231 226    H,L=-13   8    H,L= -6   8      7  32 -39    H,L=-11   9      3  57  50      4  27 -12      9  43 -35      3  61  64
   5  37  16      5  76  81      3  40  31      9  29 -30      1  47  36      9  58 -58     11  28 -26      0  94 -94      7  32 -25
   7  66  78      7  63 -52    H,L=-12   8      4  21   3     11  32 -37      3  48 -43    H,L= -2   9      0  56 -46      2  25 -18      9  30 -19
   9  54 -56      9  36 -35      0  56 -62      2  24  24      8  26  29    H,L=-10   9    H,L= -2   9      1  32  15    H,L= -1  11      8  36  24
  11  37 -50     13  32 -17      2  24  24     10  38  30     12  26 -30      2  32 -25      4  56  58      3  48 -49      1  44  41      3  37 -35
H,L= -4   7    H,L=  2    7    H,L=-11   8      1  35  31      1  25  25      4  71 -72    H,L= -1   9      5  34 -37    H,L= -1  11
   2 221-205      4  38 -34      6  32  34      3  31  30      3 114 117    H,L= -9   9      1  30 -28    H,L= -8  10      2  10    H,L=-12  12
   4  52 -50      6  32  34      8  51  52      7  34 -37      5 100 -93      7  54 -39      3 100 -96      0  40  36    H,L= -2  10      0  29  17
   8 102  94      8  51  52     10  24   4      9  64 -65      7 103-110      9  35 -31      5  42 -41      4  32  32      0  33  24      6  25 -22
  10  89  79     10  24   4    H,L=  3    7    H,L=-10   8     11  31  31     11  28  -1      7  27 -34      6  55 -50    H,L= -3  10
  14  36 -38     14  26 -15      1  29 -19     13  29  24      0  63  61    H,L= -8   9      6  29 -30      8  29 -30      1  29 -31      0  47 -41
H,L= -3   7    H,L=  3    7      3 146-147      3 125-121    H,L=-10   8      7  57  58     11  37  33    H,L= -7  10      3  26  -8      0  29 -22
   1  41 -25      5  45 -43    H,L=-10   8      2  43 -37      0 114 120      8  29 -33    H,L=-15  11      3  30   9    H,L= -5  12
   3 146-147      7  29  18      4  84  80      4  34  46      2  52  46      3  49  46    H,L= -5  12
   5 101  97    H,L= -2   7      2 194 182      6  26 -13      4  95  95      6  85 -88    H,L= -6  10      5  58  53    H,L=-13  11      5  24 -13
   7  88 -91      4 130 125    H,L=-10   8      8  59 -63      8  29 -33      0  34 -28    H,L=-10  11      7  47 -16
  13  36  34      6  36  40     10  58 -54     10  85 -89      1  74 -68      7  29 -31      3  59  54      2  26 -27      2  28  21    H,L= -4  12
H,L= -2   7      6 119 133      8  47 -45    H,L= -9   8    H,L= -3   8      5  45  45      9  53  49      7  35  33      8  29 -20      0  39 -25
   2 194 182     10 120-124     12  74 -11      3  26 -30      3  44 -53      7  42  45     13  28  32      3  24 -13      1  34  29    H,L=-10  13
   4 127 123    H,L= -1   7      7  39  36      5  33 -27    H,L=  4    8    H,L= -6   9    H,L=  2   9      5  42 -32      3  49  43    H,L= -8  11
   6 119 133      1 148-150      9  34  -5      7  56  67      7  99 101      0  49  49      2 105-104      7  49 -47    H,L= -8  11      4  25   3
  10 120-124      3  88 -85    H,L= -6   7     11  34 -30     11  33 -21      4  73  63      6  26  10    H,L= -4  10      2  35 -26    H,L= -9  13
  12  43 -39      5  37 -39    H,L= -8   8     13  39 -41    H,L=  5    8      6  27  -6      8  28  10      5  30 -18    H,L= -7  11      5  24  18
H,L= -1   7      7 116 111      4  71 -65    H,L= -2   8      1  48  57     10  30 -22    H,L= -3   9     12  38 -30      1  29 -26
   1 148-150      9  44  37      6  35 -12      0 144 140    H,L= -2   8      5  42 -40    H,L= -5   9    H,L= -3  10    H,L= -6  11
   3  88 -85     11  35  33      8  27  21      2  79  78      0 135 128      7  45 -35      1  86 -83      2  49  50      1  33 -39      4  36  43
```

Table 5.   Observed and calculated structure factors (× 10) for the photographic data

Table 5.   (continued)

```
  K  FO  FC  DF     K  FO  FC  DF     K  FO  FC  DF     K  FO  FC  DF     K  FO  FC  DF     K  FO  FC  DF     K  FO  FC  DF

  1 329 361 -32     2 421 425  -4     2 209-220  11     4  85 -82  -3     2  45 -53   8   H,L=  0   6         3 221 182  39
  3 286 288  -2     4 498-478 -20     4 157 166  -9     6   0  -9   9     6  27  26   1     0  89 -80  -9   H,L= -4   7
  5  77  71   6     6 128-129   1     6 134 129   5   H,L= -3   5       H,L=-11   6         2 108-132  24     2 144-149   5
  9   0 -15  15     8 128-128   0     8  60  60   0     1  48 -34 -14     5  71 -69  -2     4  83  83   0     6   0  -2   2
 11  43 -49   6   H,L= -3   4        10  27 -32   5     3 104-101  -3     7  47 -36 -11     6   0  -4   4   H,L= -3   7
H,L=  6   3         1  47  46   1   H,L=  5   4         5 372-406  34   H,L=-10   6         8 119 120  -1     3 132-117 -15
  4  62 -57  -5     3  96  89   7     3 121 109  12     7   0   2  -2     0  44 -34 -10   H,L=  1   6         5  64  67  -3
  6   0 -15  15     5  81  83  -2     7  74 -65  -9    11  66  81 -15     2   0  10 -10     1  68 -57 -11   H,L= -2   7
H,L=  7   3         7  62  48  14     9  28 -34   6   H,L= -2   5         4  59  60  -1     3 115-114  -1     2 125 134  -9
  1 107-128  21    13  52 -50  -2   H,L=  6   4         2 216 219  -3   H,L= -9   6         5   0 -10  10     4  88  93  -5
  3  51 -53   2   H,L= -2   4         0  57  53   4     4 242 256 -14     1  86-113  27     7  97  98  -1     6  90  96  -6
H,L=  8   3         0 204-203  -1     2  97 103  -6     6  51 -44  -7     3  57 -48  -9     9  35  44  -9   H,L= -1   7
  2  55  60  -5     2 452-398 -54   H,L=  7   4         8 184-148 -36     5 136 129   7   H,L=  2   6         1  92-111  19
  6  54  70 -16     4 357 331  26     1  76 -86  10   H,L= -1   5       H,L= -8   6         2  87 104 -17     3  81 -60 -21
H,L=-13   4         6  76  71   5     5  54  56  -2     1 226-232   6     0  61 -65   4     4  58 -58   0     7  76  81  -5
  3  45  45   0     8 182 190  -8   H,L=-13   5         5 156 167 -11     2  52  51   1     8  80 -85   5   H,L=  0   7
H,L=-12   4       H,L= -1   4         1  37 -49  12   H,L=  0   5         4  79 -71  -8   H,L=  3   6         6  60 -69   9
  0  31 -24  -7     1 246 230  16     3  36 -34  -2     2 261-270   9     6   0 -15  15     1  87 -93   6     8   0  -7   7
  6  29  31  -2     3 420 387  33   H,L=-12   5         4 381-387   6   H,L= -7   6         3   0  12 -12   H,L=  1   7
H,L=-10   4         5 167-152 -15     2  39 -50  11     8 129 125   4     1  61  94 -33     5  71  75  -4     3 168 165   3
  0 193 184   9     7 318-298 -20     6  34 -33  -1    10   0  -4   4     5  94 -93  -1   H,L=  4   6         5  55  60  -5
  2 100 105  -5   H,L=  0   4       H,L=-11   5       H,L=  1   5         7   0   2  -2     0 169-159 -10     7  40 -37  -3
  4 141-120 -21     0  77  60  17     1  68  95 -27     1 139 142  -3   H,L= -6   6         2  43 -48   5     9  17 -24   7
  6   0  -2   2     2 120 111   9     3   0   1  -1     3  76  60  16     0   0 -15  15     4  34  35  -1   H,L=  3   7
  8  55 -62   7     4  75  77  -2   H,L=-10   5         5 139 149 -10     2 179-173  -6     6  34  41  -7     1   0 -11  11
H,L= -9   4         6 161 140  21     4  96 -91  -5     7 121-110 -11     6  72  62  10   H,L=  5   6         3  78 -86   8
  3 134-129   5     8 171-169  -2     6  48 -44  -4     9  77 -67 -10   H,L= -5   6         1  65  70  -5   H,L=  4   7
  7  64  57   7    12   0  12 -12   H,L= -9   5        11  27 -27   0     1  56  69 -13     5  49 -56   7     4  71  81 -10
 11  43 -41  -2   H,L=  1   4         7 119-126   7   H,L=  2   5         3 161-158  -3   H,L=  6   6       H,L=-12   8
H,L= -8   4         1 227-215 -12   H,L= -8   5         2  78  92 -14     5  70 -49 -21     0  54  54   0     0  29 -35   6
  0   0 -13  13     3 128-126  -2     2 111 113  -2     4 130 131  -1     7   0  -2   2   H,L=-12   7         2   0  11 -11
  4 147 125  22     5 198 194   4     4  71  70   1     6  59 -35 -24   H,L= -4   6         2  66  65   1   H,L=-10   8
  6  68 -59  -9     7 202 196   6    10  63 -73  10     8  47 -45  -2     0  80  65  15   H,L=-11   7         0   0  10 -10
H,L= -7   4         9  44  56 -12   H,L= -7   5       H,L=  3   5         2 133 151 -18     3  50  48   2     4  50  44   6
  3   0   0   0    11  46 -44  -2     3 185-167 -18     1  92 -89  -3     4   0 -10  10   H,L=-10   7       H,L= -8   8
  7 148-156   8    13  28 -35   7     5  70 -53 -17     3 113-100 -13     6 104-103  -1     2  47 -48   1     0  91  89   2
  9 163-153 -10   H,L=  2   4         7 152 160  -8     5 237-240   3   H,L= -3   6       H,L= -9   7         2  45  46  -1
H,L= -6   4         0 245 258 -13   H,L= -6   5         9  46  58 -12     1 309-367  58     1  40  41  -1     4  51 -49  -2
  0 363-366 -17     2 310 327 -17     2 302-304   2   H,L=  4   5         3 174 151  23     5  48  47   1     6  75 -69  -6
  4 232 195  37     4 151-158   7     4  92-108  16     6   0  -1   1     5 180 178   2   H,L= -8   7       H,L= -7   8
  6  72  68   4     6 254-238 -16     6  69 -76   7     8  50 -43  -7   H,L= -2   6         2   0  10 -10     5  51  50   1
  8   0  -2   2     8   0   7  -7     8   0   0   0   H,L=  5   5         0  92 -93   1     6  96 101  -5   H,L= -6   8
 10  70 -68  -2    12  35 -32  -3    10   0   2  -2     3  54  45   9     2  71 -74   3   H,L= -7   7         0 126-137  11
 12  56 -62   6   H,L=  3   4       H,L= -5   5       H,L=  6   5         4  94-100   6     1  84-105  21     6  71  59  12
H,L= -5   4         1 284 263  21     1 251 264 -13     2 122-145  23     6 107 109  -2     3  61 -44 -17   H,L= -5   8
  3 115-122   7     3  72 -78   6     3 138 127  11     4  64 -72   8   H,L= -1   6       H,L= -6   7         3  87  81   6
  7  90 114 -24     5  60 -65   5     5 161 170  -9   H,L=-13   6         1 217 230 -13     2  94  98  -4     5  65 -61  -4
  9 107 124 -17     7   0   1  -1     7 159-160   1     3   0 -16  16     3   0 -15  15     6  70 -69  -1     7  66 -67   1
H,L= -4   4       H,L=  4   4        11  70 -77   7   H,L=-12   6         5 144-147   3   H,L= -5   7       H,L= -4   8
  0 821 795  26       165-155 -10   H,L= -4   5         0  37  38  -1     7 115 -96 -19     1 121 151 -30     0  77  84  -7
```

Table 5.   (continued)

K	FO	FC	DF		K	FO	FC	DF		K	FO	FC	DF		K	FO	FC	DF		K	FO	FC	DF		K	FO	FC	DF		K	FO	FC	DF
4	64	66	-2		4	83	-82	-1		5	0	-4	4		3	55	40	15		4	67	-72	5		0	0	-10	10		0	0	-12	12
6	0	2	-2		6	65	-57	-8		H,L= 0					H,L= 1					H,L= 3					H,L= 0					H,L= 0			
H,L=					H,L= 1					0	2	8	-6		1	38	49	-11		3	42	26	16		0	23	-19	-4		0	-2	10	-2
1	46	-65	19		1	59	82	-23		4	36	42	-3		3	52	-45	-7		5	0	-6	6		1	-7	10					39	41	
5	61	56	5		H,L= 0					4	29	32	9		5	51	-55	4		H,L= 2					3	30	-43	13					
7	59	65	-6		0	107	-111	4		H,L=-11					H,L= 1					2	36	40	-4		5	34	28	6					
H,L=					4	43	39	4		3	28	-24	-4		1	38	-54	16		H,L=					5	30	29	1					
0	90	91	-1		H,L= 3					H,L=-10					H,L= 1					2	22	27	-5		H,L=								
2	42	55	-13		3	0	-8	8		4	33	-41	8		2	62	-69	7		4	0	-8	8		1	28	39	-11					
										H,L= -9															2	-4	10							
											-9	9																						

Fig. 1. A composite drawing of the final electron-density map, viewed along b-axis. Contours are drawn at intervals of 4 e.$\mathring{A}^{-3}$ for the chlorine atom and 2 e.$\mathring{A}^{-3}$ for the other atoms, beggining with 2 e.$\mathring{A}^{-3}$.
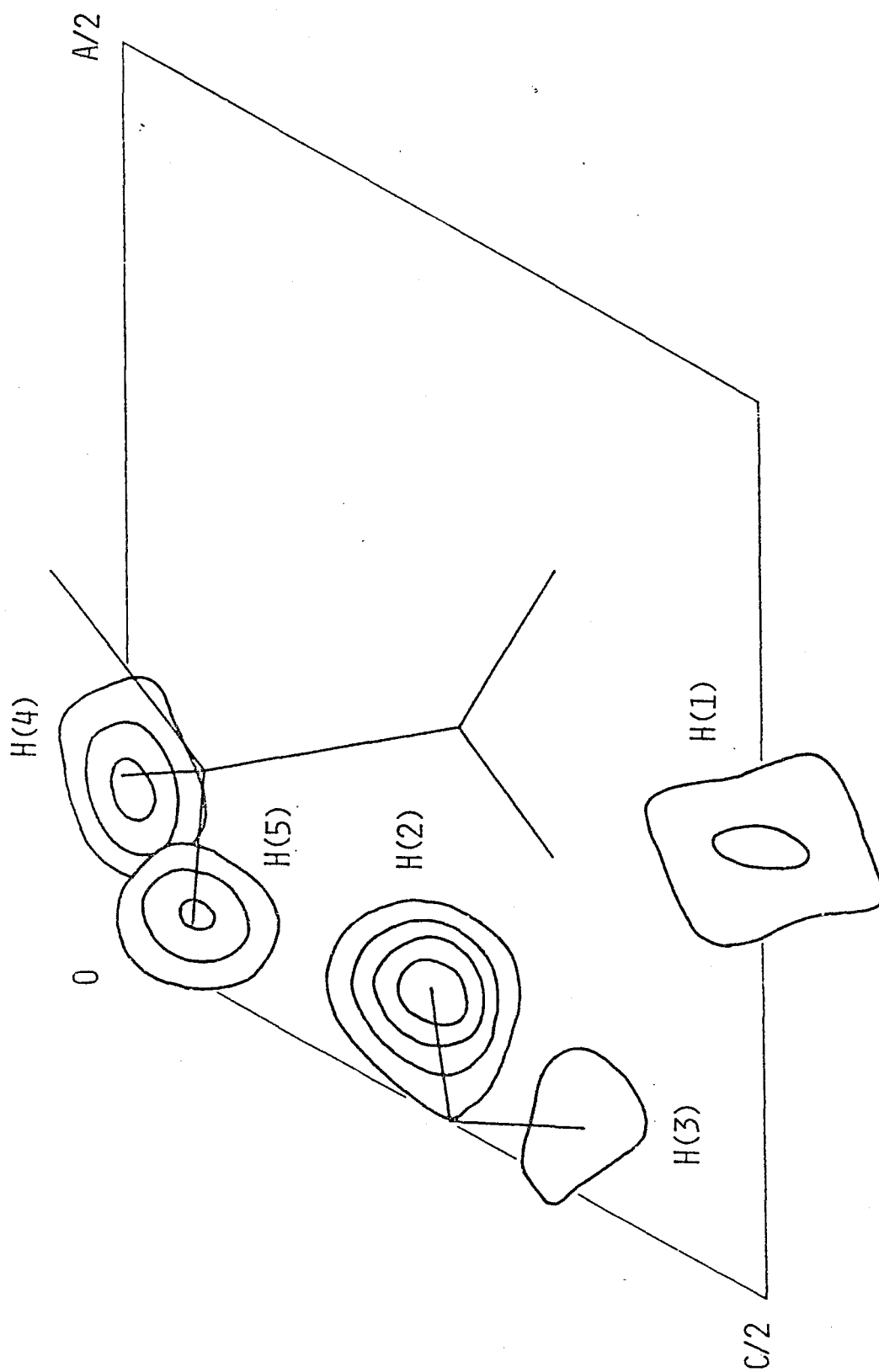
Fig. 2. A composite drawing of the final difference electron-density map, viewed along b axis. The contribution of the hydrogen atoms were excluded from the calculated structure factors. Contours are drawn at intervals of 0.1 e.Å^{-3}, beginning with 0.2 e.Å^{-3}.

Fig. 3. The structure viewed along a axis. The crystallographically symmetrical hydrogen bonds are shown by broken lines.

◎ Cl ◯ O ○ N ◯ C ○ H'
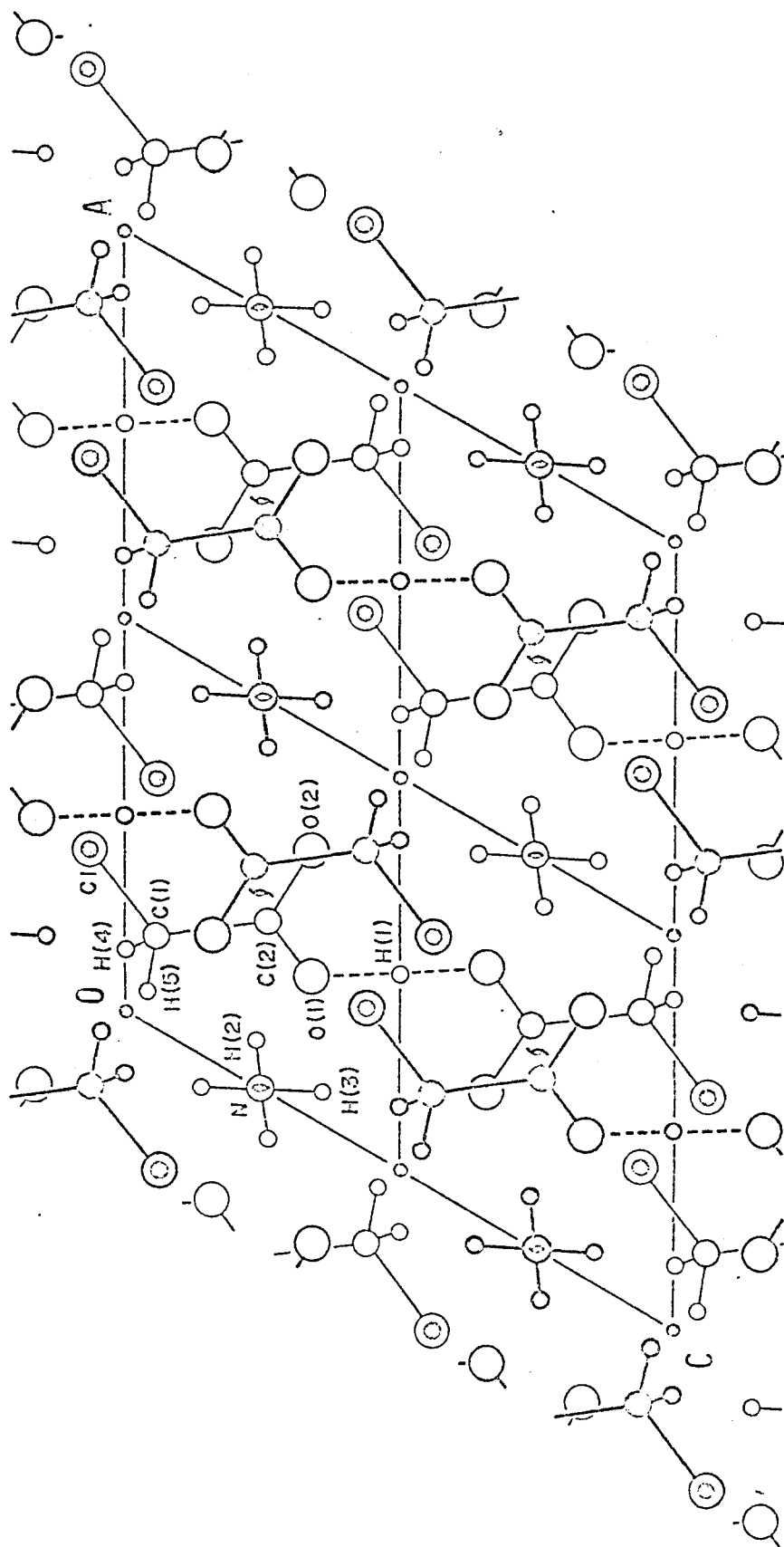
Fig. 4. The structure viewed along b axis.

Table 6. Summary of the inter-carboxyl hydrogen bonds in some Type A acid salts of monocarboxylic acids, MHX_2.

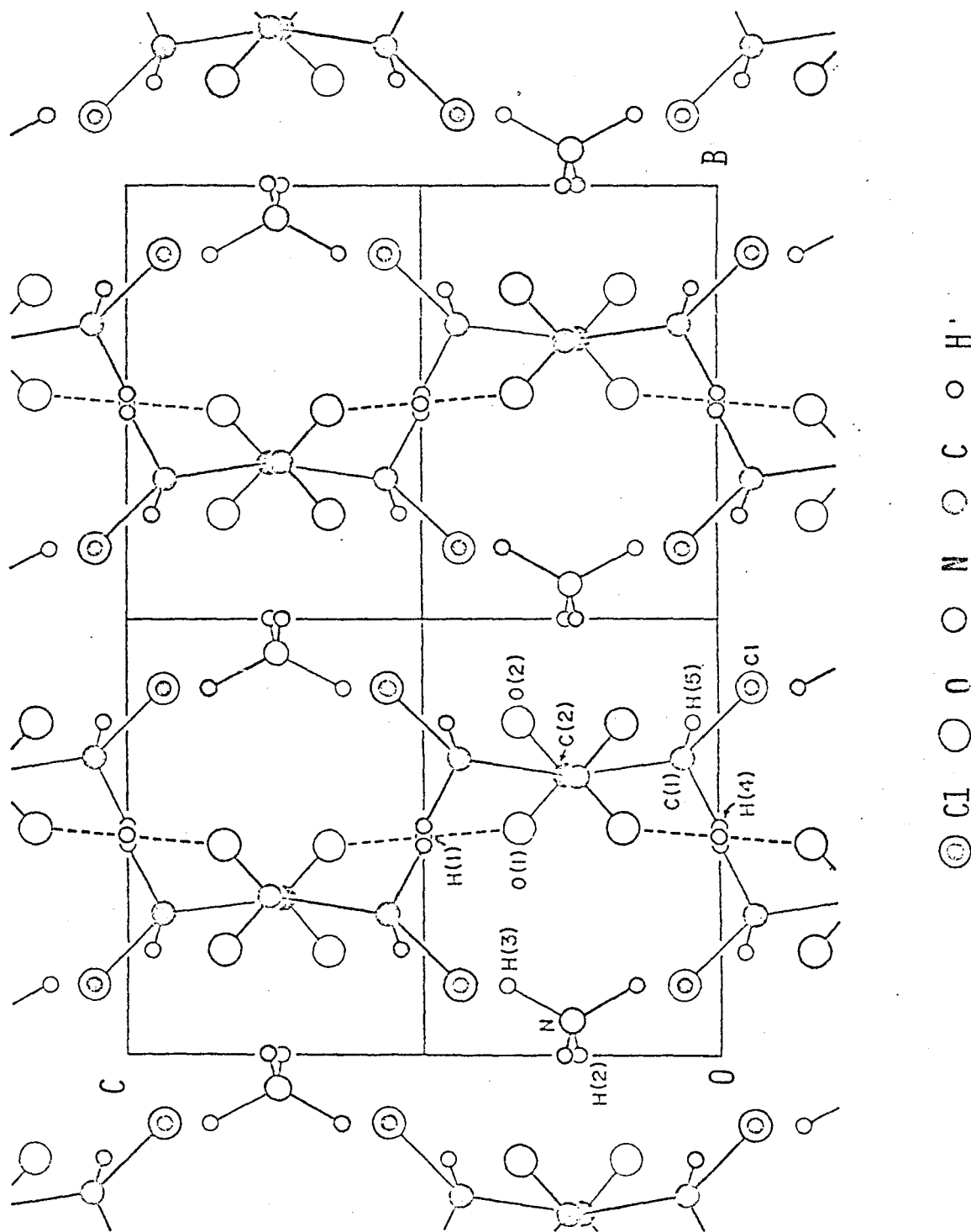| HX	M	space group	Mole-cules per cell	Sym-metry of bond	O...H...O		Ref.
phenylacetic	K	I2/a	4	$\bar{1}$		2.443(4)	11
benzoic	K	C2/c	4	$\bar{1}$		2.51(4)	12
p-HO-benzoic	K	P/2c	2	$\bar{1}$		2.458(6)	13
acetic	Na	Ia3	24	2	(X)	2.444(10)	14
					(N)	2.475(14)	15
cinnamic	NH_4	C2/c	4	$\bar{1}$		2.51(3)	16
p-Cl-benzoic	K	C2/c	4	$\bar{1}$		2.457(13)	17
m-Cl-benzoic	K	C2/c	4	$\bar{1}$		2.437(6)	18
trifluoro-acetic	Cs	A2/a	4	$\bar{1}$		2.38(3)	19
	K	C2/c	4	$\bar{1}$	(X)	2.435(7)	19
					(N)	2.437(4)	20
	K	C2/c	4	$\bar{1}$	(X)	2.455(5)	21
aspirin					(N)	2.448(4)	22
	Rb					2.48(2)	23
$O-NO_2$-benzoic	Rb	$P\bar{1}$	1	$\bar{1}$		2.43(6)	10
anisic	K	Rbcn	4	2		2.476(18)	24

The ammonium ion

The ammonium ion lies on a twofold axis surrounded by oxygen atoms from six different carboxyl groups, making hydrogen bonds with them. The interatomic distances and angles of the ammonium ion and the hydrogen bond are listed in Table 7. The atom H(2) is adjacent to the atom $O(2^{iv})$, while H(3) is adjacent to $O(2^{i})$ and O(1).

The chloroacetate residue

The best plane of the carboxyl group and C(1) is represented by the equation

$$-0.6279\ X + 0.7488\ Y + 0.2121\ Z = 2.4190\ ,$$

where the direction cosines are referred to the orthogonal axes a, b and c*, and X, Y and Z are expressed in Å.
The deviations of the atoms from the plane are:
O(1)   0.003, O(2)   0.004, C(1)   0.003, C(2)   -0.010 Å
The Cl atom lies 0.21 Å out of the plane.

The bond lengths and angles in the chloroacetate residue are presented in Table 7 and Fig.5. The Cl-C(1) bond length of 1.768 Å is in good agreement with the value of 1.767 Å given by Sutton.[25] The bond length of C(1)-C(2), 1.506 Å, agrees with that found in other Type A acid salts and also with that given by Sutton.[25] The C-O bond lengths are 1.278 Å for C(2)-O(1) and 1.225 Å for C(2)-O(2), and the C-C-O angles are 111.4° for C(1)-C(2)-O(1) and 123.2° for C(1)-C(2)-O(2).

Table 7. Interatomic distances and bond angles with
their standard deviations

The e.s.d.'s given in parentheses refer to the last figure.

ammonium ion

N	-	H(2)	1.01(4) Å	H(2)	- N	-	H(2^{ii})	110(4)°
N	-	H(3)	0.86(3)	H(2)	- N	-	H(3)	115(3)
				H(2)	- N	-	H(3^{ii})	99(4)
				H(3)	- N	-	H(3^{ii})	121(5)

chloroacetate residue

C(1)	- Cl	1.768(4)	Cl	- C(1)	- C(2)	113.4(2)
C(1)	- C(2)	1.506(4)	C(1)	- C(2)	- O(1)	111.4(2)
C(2)	- O(1)	1.278(4)	C(1)	- C(2)	- O(2)	123.2(3)
C(2)	- O(2)	1.225(3)	O(1)	- C(2)	- O(2)	125.4(3)
C(1)	- H(4)	0.96(3)	Cl	- C(1)	- H(4)	104(3)
C(1)	- H(5)	0.99(5)	H(4)	- C(1)	- H(5)	111(3)
			H(5)	- C(1)	- Cl	109(2)
			H(4)	- C(1)	- C(2)	112(2)
			H(5)	- C(1)	- C(2)	108(2)

hydrogen bond

N	...O(2^{iv})	2.880(3)	N	- H(2)...O(2^{iv})	163(3)
H(2)...O(2^{iv})	1.90(4)	N	- H(3)...O(2^{i})	161(3)
N	...O(2^{i})	3.148(3)	N	- H(3)...O(1)	108(3)
H(3)...O(2^{i})	2.32(3)			
N	...O(1)	2.926(4)	C(2) - O(1)...O(1^{i})	114.8(3)
H(3)...O(1)	2.55(4)			
O(1)...O(1^{i})	2.432(5)			

Superscripts refer to atoms at :

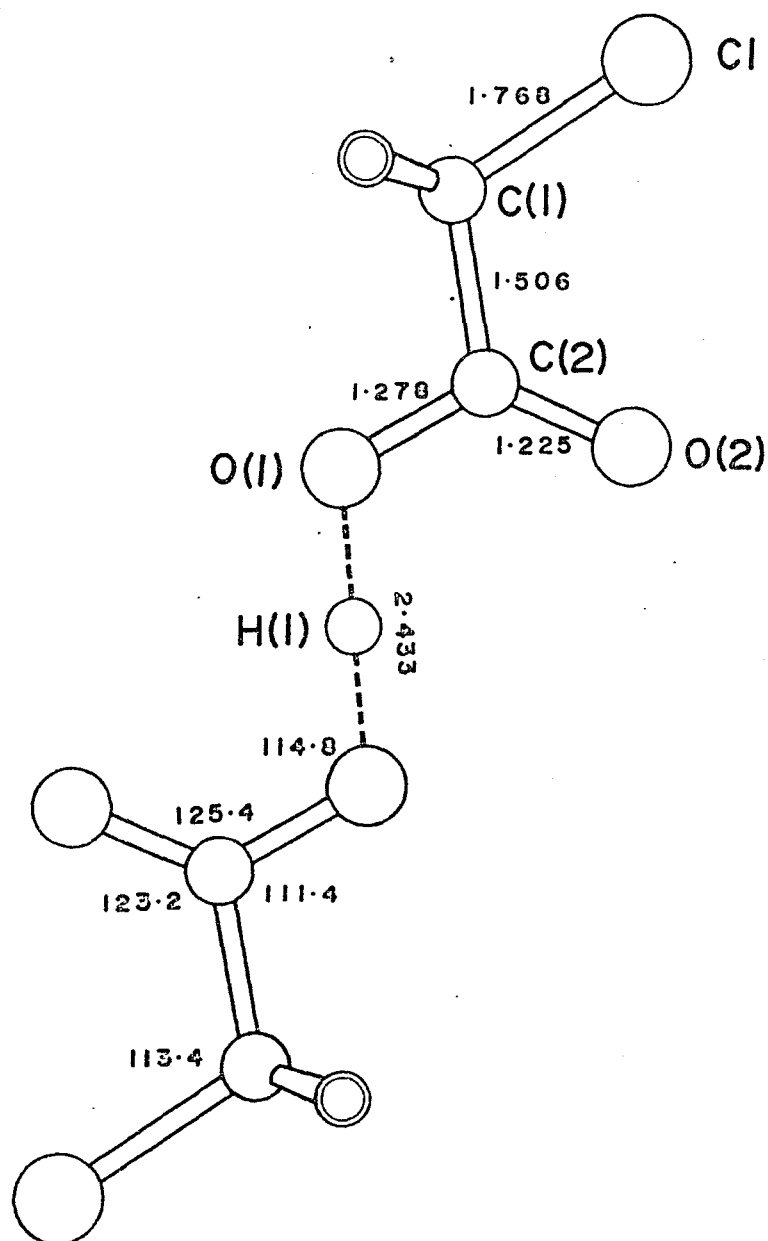|				
i	1/2-x, 1/2-y, 1-z	iii	-x, y, -1/2-z
ii	-x, y, 1/2-z	iv	1/2-x, -1/2+y, 1/2-z

Fig. 5.　Bond distances and angles in the chloroacetate residue.

It is pointed out that in the fully ionized carboxyl group the two C-O bond-lengths and the two C-C-O angles are equal, while in un-ionized carboxyl group they differ.[26] The difference of the bond-lengths, 0.053 Å, and the deviation of the angles from 118° seem to indicate that the carboxyl group in ammonium hydrogen bis (chloroacetate) is intermediate in character between fully ionized and neutral, as is pointed out in the study of other Type-A acid salts.[11,13] It should be noted here that this character is caused by the very short hydrogen bond[27] described below. The distance of Cl-Cl^{iii}, 3.604 Å, is nearly equal to the sum of van der Waals radii. There is no abnormal intermolecular contact.

II.5. The very short hydrogen bond

The chief interest in $NH_4H(ClCH_2COO)_2$ lies in the crystallographically symmetric hydrogen bonds $O(1)...O(1^i)$, which are shown by broken lines in Figs.3 and 4. As in most Type A acid salts (Table 6), symmetry element affecting the hydrogen bond is a center of symmetry which requires the proton to be exactly at the mid-point between the oxygen atoms.

However, X-ray analysis cannot distinguish between the two cases: (a) the case in which the proton vibrates in a symmetric single-minimum potential well at

the mid-point, and (b) the case in which it is distributed
at random in a set of symmetric double-minimum well,
situated close to either side of the mid-point. Even with
the neutron diffraction analysis which is more powerful
method than X-ray for studying the location of hydrogen
atoms, it is difficult to distinguish definitely the
two cases. It is shown in the case of $NaHF_2$ by McGaw and
Ibers[28] that it is equally possible to interprete the
observed scattering density by the case (a) or by the
case (b). Meanwhile it is known that crystals having a
very short and possibly symmetric hydrogen bond show anomalous
infrared spectra, although the assignment of each band does
not seem to have been established enough. There is a
remarkably intense background absorption over several
hundred cm^{-1} of which the maximum lies between 700 and
900 cm^{-1}, with various peaks and often with a
transmission 'window' in it.[2]

It has been pointed out by McGaw and Ibers[28] that a
combination of diffraction and spectroscopic data, i.e.
comparison of r.m.s. amplitude of thermal motion derived
from both data, provides the most powerful evidence that
FHF hydrogen bond in $NaHF_2$ has the potential of
single-minimum type. In Type A acid salts, the precise
neutron diffraction results in potassium hydrogen
bis (trifluoroacetate)[20] and potassium hydrogen
bis (aspirinate)[22] were analysed along this line.

Thermal vibration ellipsoids of OHO group contain

some overall motion which are causing oxygen and hydrogen

atoms to move in the same direction. A more useful

information may be obtained by subtracting the oxygen

atom motion from the hydrogen atom motion: $U_\Delta = U_H - U_O$.

The difference ellipsoid is strikingly elongated along

the OHO bond, and indicates that the major motion of the

hydrogen atom is along the bond. The difference ellipsoid

should closely approximate the motion of the hydrogen

atom in a static field of two motionless oxygen atoms;

in particular the amplitude along the bond should be

closely related to the asymmetric stretching frequency of

the idealized OHO system. The U_Δ values of 0.19 (0.17) $\overset{o}{A}$

for KH (aspirinate)$_2$ (KH(CF$_3$COO)$_2$) were obtained along the

bond from the difference ellipsoid. On the other hand,

the asymmetric stretching frequency in both compounds are

assigned to 800 cm^{-1}.[20,29] If a simple harmonic motion

of a particle with mass 1 is assumed, the r.m.s. amplitude

of 0.14 $\overset{o}{A}$ is derived. The difference $U_\Delta - U_{IR}$ 0.05

(0.03) $\overset{o}{A}$ for KH (aspirinate)$_2$ (KH(CF$_3$COO)$_2$) are not large

and are plausibly accounted for some departure of the

hydrogen atom potential functions from a simple harmonic

one., i.e. anharmonicity. If a double-minimum potential

well is assumed, and the difference $U_\Delta^2 - U_{IR}^2$ is ascribed

to the displacement of an equilibrium point from the

center, the values of 0.13 (0.09) $\overset{o}{A}$ are obtained for

KH (aspirinate)$_2$ (KH(CF$_3$COO)$_2$), which are less than

0.14 $\overset{o}{A}$ of U_{IR}. Thus the double-minimum model leads to

that a half-hydrogen atom undergoes a simple harmonic

motion with a r.m.s. amplitude of 0.14 $\overset{\circ}{A}$ around the

equilibrium position displaced 0.13 (0.09) $\overset{\circ}{A}$ from the

mid-point of the OHO bond in KH (aspirinate)$_2$ (KH(CF$_3$COO)$_2$);

the r.m.s. magnitude of 0.14 $\overset{\circ}{A}$ from one of the assumed

equilibrium points would bring the hydrogen atom from

one well to the other. Therefore it is concluded that

the hydrogen motion can be described in terms of a broad,

flat anharmonic potential, possibly with a hump below

zero-point vibrational level, i.e. that the hydrogen atom

potential is effectively of single-minimum type.

The very short hydrogen-bond lengths in NH$_4$H(ClCH$_2$COO)$_2$

is 2.432 $\overset{\circ}{A}$, which is one of the shortest among those of

Type A acid salts determined precisely with the estimated

standard deviations equal to or less than 0.010 $\overset{\circ}{A}$

(Table 6). The infrared spectrum of NH$_4$H(ClCH$_2$COO)$_2$ was

measured at room temperature, which is shown in Fig.6.

The expected anomalies common to other Type A acid salts

were found: the very broad and strong absorption lies in

the region of 400-1600 cm^{-1} with its maximum at about

900 cm^{-1}.

Therefore it can be concluded that the hydrogen atom

potential of the very short hydrogen bond of NH$_4$H(ClCH$_2$COO)$_2$

is effectively of a single-minimum type, at least to same

extent as other Type A acid salts from the following points:

(i) the hydrogen-bond length 2.432 (5) is one of the
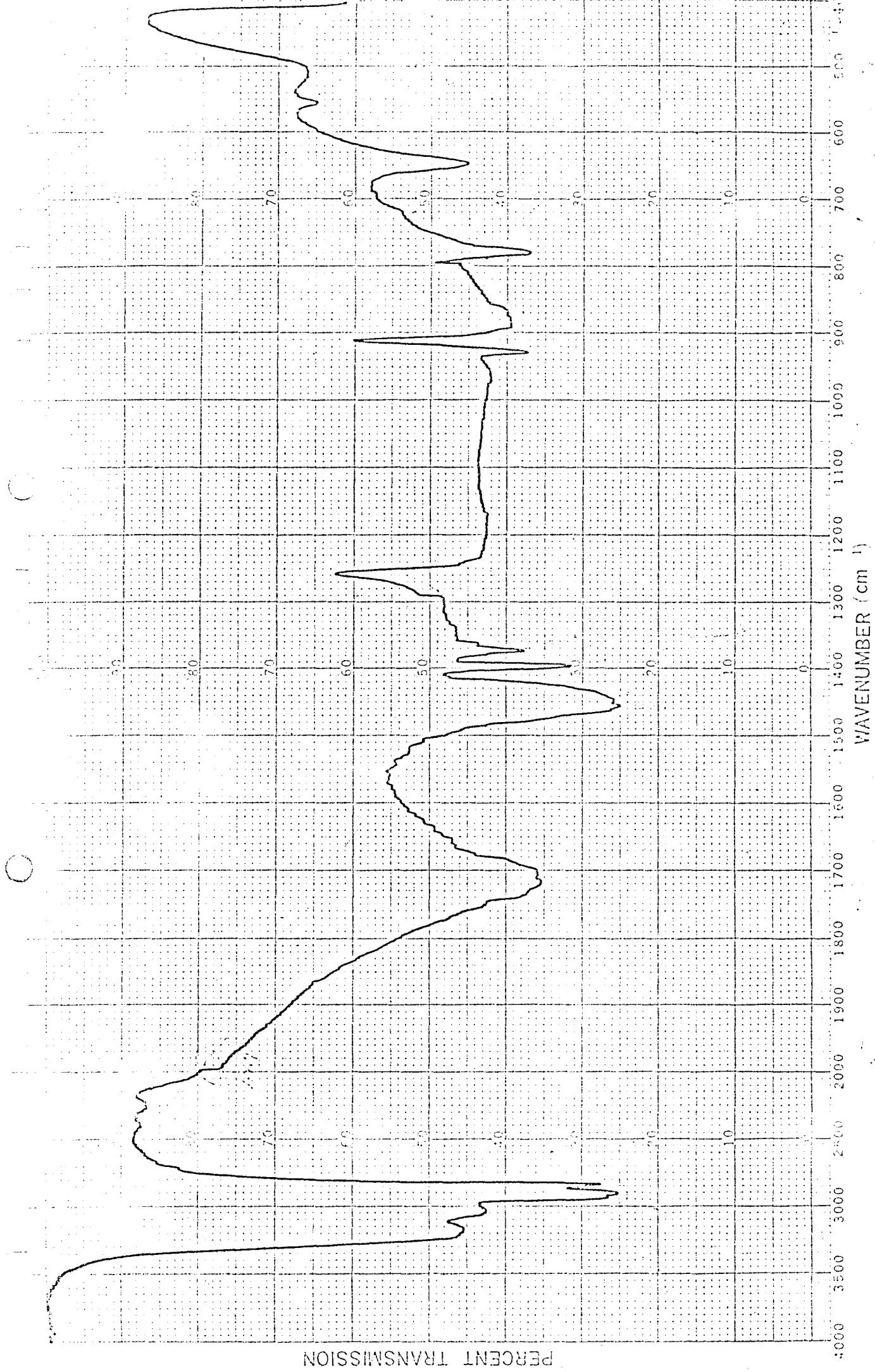
shortest among Type A acid salts, (ii) the infrared

Fig. 6. The infrared spectrum of $NH_4H(ClCH_2COO)_2$ at room temperature (Nujol).

44

spectrum at room temperature has anomalous characteristic

common to Type A acid salts, (iii) the hydrogen-bond

lengths in Type A acid salts are concentrated around mean

of six most precise values 2.445 $\overset{\circ}{A}$, in spite of much

varieties of chemical surroundings (Table 6), (iv) in

Type A acid salts, the conclusions concerning the shape of

the potential from diffraction and spectroscopic data

are in agreement with the opinion of being effectively of a

single-minimum type.[2]

Ferroelectric $NH_4H(ClCH_2COO)_2$ has the shortest

hydrogen-bond among hydrogen-bonded ferroelectrics

precisely measured until now, as far as the author is

aware, and offers the first example of hydrogen-bonded

ferroelectrics with a single-minimum potential well.

Occurence of a ferroelectric with a single-minimum

potential well is of a particular significance, because

the phase transition mechanism in hydrogen-bonded

ferroelectrics with short hydrogen bonds is ordinarily

considered on the basis of the order-disorder model such

as KH_2PO_4, where the shape of the potential is assumed

to be of double-minimum type, and the hydrogen atom in

the OHO bond cannot play a crucial role as trigger of

phase transition in a single-minimum potential well.

Ferroelectric $NH_4H(ClCH_2COO)_2$ seems to give a new clue to

unified understanding of hydrogen-bonded ferroelectrics,

which are full of variety, from structural

characteristics of hydrogen bonding.

References

1) M. Ichikawa and T. Mitsui: Phys. Rev. 152 (1966) 495.

2) J. C. Speakman: chem. Commun. (1967) 32;

   Structure and Bonding 12 (1972) 141.

3) M. Ichikawa: Acta Cryst. B28 (1972) 755.

4) International Tables for X-ray Crystallography

   (Kynoch Press, Birmingham, 1959 and 1962)

   Vol.II and Vol.III.

5) D. C. Phillips: Acta Cryst. 9 (1956) 819.

6) J. S. Rollett and R. A. Sparks; Acta Cryst.

   13 (1960) 273.

7) A. J. C. Wilson: Acta Cryst. 2 (1949) 378.

8) UNICS Universal Crystallographic Computing System,

   ed. T. Sakurai (Crystallographic Society of Japan,

   1967).

9) M. J. Buerger: Crystal-structure analysis

   (John Wiely & Sons, New York, 1960); H. Lipson and

   W. Cochran: The Crystalline State. Vol.III.

   The Determination of Crystal Structures,

   ed. Sir L. Bragg (G. Bell and Sons, London, 1966).

10) H. N. Shrivastava and J. C. Speakman: J. chem. Soc.

    (1961) 1151.

11) L. Manojlović and J. C. Speakman: Acta Cryst.

    B24 (1968) 323.

12) J. M. Skinner, G. M. D. Stewart and J. C. Speakman:

    J. chem. Soc. (1954) 180.

13) L. Manojlovic: Acta Cryst. B24 (1968) 326.

14) J. C. Speakman and H. H. Mills: J. chem. Soc. (1961) 1164.

15) M. J. Barrow, M. Currie, K. W. Muir, J. C. Speakman and D. N. J. White: J. chem. Soc. Perkin II. (1975) 15.

16) R. F. Bryan, H. H. Mills and J. C. Speakman: J. chem. Soc. (1963) 4350.

17) H. H. Mills and J. C. Speakman: J. chem. Soc. (1965) 4355.

18) A. L. Macdonald and J. C. Speakman: J. chem. Soc. Perkin II. (1973) 1564.

19) L. Golic and J. C. Speakman: J. chem. Soc. (1965) 2530.

20) A. L. Macdonald, J. C. Speakman and D. Hadži: J. chem. Soc. Perkin II. (1972) 825.

21) L. Manojlovic and J. C. Speakman: J. chem. Soc. A. (1967) 971.

22) A. Sequeira, C. A. Berkebile and W. C. Hamilton: J. molecular Struct. 1 (1967) 283.

23) S. Grimvall, R. F. Wengelin: J. chem. Soc. A. (1967) 968.

24) D. R. McGregor and J. C. Speakman: J. chem. Soc A. (1968) 2106.

25) L. E. Sutton: Tables of Interatomic Distances and Configuration in Molecules and Ions (The Chemical Society, London, 1965) Supplement.

26) T. Hahn: Z. Krist. 109 (1957) 438.

27) M. Ichikawa: Submitted to Acta Cryst. B (1978).

28) B. L. McGaw and J. A. Ibers: J. chem.Phys.
    39 (1963) 2677; W. C. Hamilton and J. A. Ibers:
    Hydrogen Bonding in Solids (Benjamin, New York, 1968)
    Chap.3.

29) A. Novak: Structure and Bonding 18 (1974) 177.

Chapter III.   The X-ray Crystal Structure Analysis of

    Ferroelectric $NH_4H(ClCH_2COO)_2$ of the Ferroelectric

    Phase at 80 K

III.1. Introduction

    In chapter II the results of the X-ray crystal

structure analysis of ferroelectric $NH_4H(ClCH_2COO)_2$ in the

paraelectric phase at room temperature have been described.[1]

It has been shown that $NH_4H(ClCH_2COO)_2$ has the shortest

hydrogen bond among the hydrogen-bonded ferroelectrics

precisely measured so far and it offers the first

example with the hydrogen-atom potential of a single-minimum

type. In this chapter the results of the crystal

structure analysis of the ferroelectric phase at 80 K is

described,[2] which has been carried out with an interest

in the structural change accompanying the ferroelectric

phase transition, in particular the structural changes in

the OHO bond and the NH_4^+ ion. On the basis of the

structures of the paraelectric and the ferroelectric

phase, the mechanism of the ferroelectric phase transition

is discussed together with the results of other experimental

technique mainly by chihara and coworkers; the ^{35}Cl

nuclear quadrupole resonance frequencies[3]; Raman and

infrared spectra[4] in $NH_4H(ClCH_2COO)_2$ and $ND_4D(ClCH_2COO)_2$,

the ^{35}Cl nuclear quadrupole resonance frequencies and

relaxation times in $NH_4H(ClCH_2COO)_2$,[5] heat capacity of

$NH_4H(ClCH_2COO)_2$ and $ND_4D(ClCH_2COO)_2$.[6]

III.2. Experimental

Low-temperature apparatus

The apparatus of cold-gas blowing type (Fig. 1) was
used to take low temperature Weissenberg photographs by
equi-inclination method, which was intended firstly for
helium gas,[*] but nitrogen gas was used in this study.
A Weissenberg camera is put in a box. Air in the box was
replaced with dry nitrogen gas to prevent icing of the
sample. Then liquid nitrogen was transferred to a small
cylindrical box with heaters for evapolation, by pressure
added from nitrogen bomb in addition to pressure due to
natural evaporation in a metal Dewar vessel. Cold nitrogen
gas was blowed over the sample. All data were collected
at 80 K. Stability of temperature was attained by
controlling the nitrogen gas gas flow of the bomb and the leak
valve and was maintained within $\pm$ 2°. The temperature was
measured by an Au: 2.1 % Co-Cu thermocouple placed at
about 1 mm from the crystal.

---

*) K. Itoh, Y. Shiozaki, A. Hashiguchi and T. Mitsui:
   private communication.
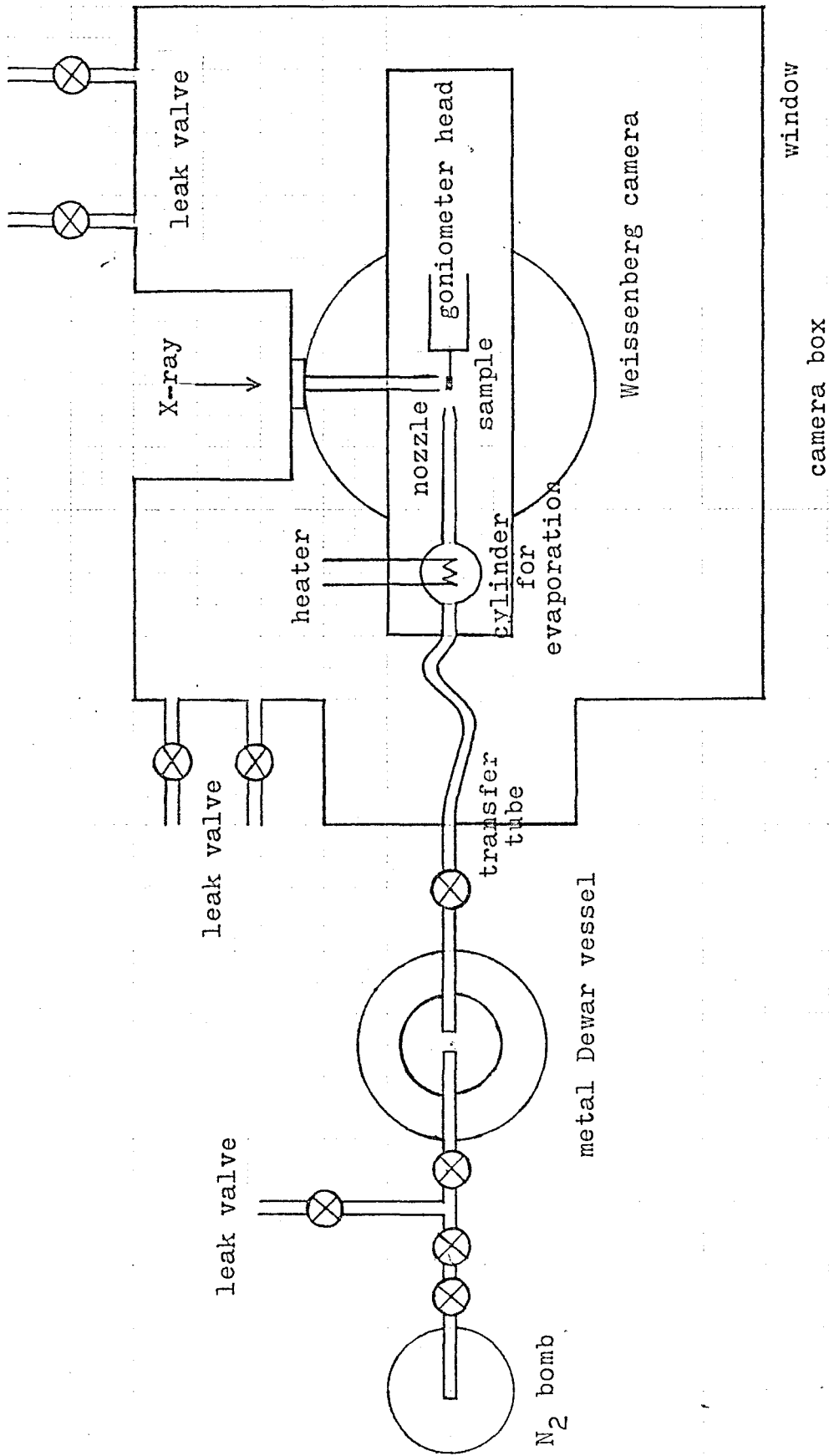
Fig. 1. A schematic diagram of the low-temperature Weissenberg camera apparatus of cold gas blowing type

Data collection and processing

Weissenberg photographs were taken with Cu Kα radiation to determine the space group and unit-cell parameters. The systematic absences of reflections are the same as those observed at room temperature and because the crystal is now polar the space group changes from C2/c to Cc. Unit-cell parameters were determined from a least-squares treatment, using θ values for 50 reflections measured on zero-layer Weissenberg photographs taken around each crystallographic axis. The systematic errors described in II.2 were considered partly by adding a $\sin 2\theta$ term in the observation equations. The crystal data are given in Table 1.

Three-dimensional intensity data were obtained from Weissenberg photographs of four multiple film taken about the a, b and c axes with Cu Kα radiation of 50 KV, 24 mA and about two and half hours exposure. Cylindrical crystals 0.38 ～ 0.42 mm in diameter with nail varnish were used. Possible efforts for obtaining accurate data were exerted in the following respects; as many photographs as possible were taken to get the reliable scaling factors and many numbers of reflections (layers: h = 0 ～ 5; k = 0 ～ 6; l = 0 ～ 4) and the integrated intensities were measured by tracing manually the spots with a Rigaku Denki Recording Microphotometer MP-3. Intensities were corrected for Lorentz, polarization, and absorption effects (μ CuKα = 63 cm^{-1}). Absorption correction factors used

Table 1.   Crystal data at 80°K

$$a = 10.47 \pm 0.02 \text{ Å}$$
$$b = 11.40 \pm 0.01$$
$$c = 8.22 \pm 0.01$$
$$\beta = 119.3 \pm 0.1°$$
$$U = 857 \pm 2 \text{ Å}^3$$

Formula : $NH_4H(ClCH_2COO)_2$

Systematic absences   hkl for h+k = 2n,

                              h0l for l = 2n

Space group   Cc

F.W.   206.0

$D_x = 1.60 \text{ gcm}^{-3}$

F(000) = 424

Z = 4

$\lambda(Cu \, K\alpha_1) = 1.5405 \text{ Å}$

$\lambda(Cu \, K\alpha_2) = 1.5443$

were taken from International Tables for X-ray
Crystallography.[7] Corrections for the elongation of
spots on the high layers were made according to
Phillips.[8] The data from each layer were correlated by
the method of Rollett and Sparks[9] and then placed on an
absolute scale by Wilson's method.[10] 647 independent
reflections including those with non-zero intensity was
obtained.

III.3. Refinement of the structure

The positional parameters obtained at room
temperature[1] and the overall temperature factor of the
low-temperature modification derived from Wilson's
method[10] were used as the initial parameters in successive
refinements. Positional parameters and individual
isotropic temperature factors were refined by a
block-diagonal least-squares method, except for hydrogen
atoms, although the contribution of hydrogen was taken
into consideration in the calculation of structure factors.
The quantity minimized was $\sum (|F_o| - 1/k|F_c|)^2$.
Refinement was continued until all parameter shifts were
less than one third their standard deviations. In the
final cycle, those reflections that were unable to be
detected, but which had calculated structure factor less
than the minimum observable values, were included in the

computation. Six strong reflections were excluded, because they are probably affected by extinction. The damping factor of 0.8 was applied to the shifts of all parameters. The final R was 0.106 (0.097 if undetectably weak reflections were excluded). The atomic scattering factors were taken from International Tables for X-ray Crystallography.[7]

All the calculations were made on a FACOM 230-60 computer with UNICS.[11] The final positional parameters and temperature factors are given in Table 2 together with their standard deviations and the table of $|Fo|$ and $|Fc|$ is in Table 3.

III.4. Description of the structure

General view

The structure viewed along the b axis is shown in Fig.2. Structural changes, due to symmetry change accompanying the ferroelectric phase transition, are as follows. The nitrogen atom which occupies the special position on a two fold axis in the paraelectric phase is now located at the general position. The two chloroacetate radicals (abbreviated CA(1), CA(2)) become non-equivalent and the acidic hydrogen atom which connects the two radicals is not necessarily exactly at the mid-point between two oxygen atoms. The correspondence between atomic

Table 2. The atomic positional parameters ($\times 10^4$) and the temperature factors at 80°K with their standard deviations

	x	y	z	B ($\overset{\circ}{A}{}^2$)
Cℓ(1)	1864(4)	4276(3)	-687(6)	1.57(5)
Cℓ(2)	3150(4)	797(3)	10733(6)	1.76(6)
O(11)	1663(11)	2527(9)	3162(15)	1.70(18)
O(12)	3412(12)	3679(10)	3312(16)	2.01(19)
O(21)	3179(12)	2446(10)	6572(16)	2.16(20)
O(22)	1600(10)	1175(8)	6693(14)	1.03(15)
N	0(17)	440(9)	2791(18)	1.44(20)
C(11)	1174(17)	3416(14)	458(23)	1.84(26)
C(12)	2164(13)	3240(11)	2421(18)	0.68(19)
C(21)	3915(16)	1622(12)	9495(21)	1.48(24)
C(22)	2723(15)	1713(13)	7350(20)	1.25(22)

As for numbering of atoms, see Table 4.

Table 3. Observed and calculated structure factors

K	FO	FC	K	FO	FC	K	FO	FC	K	FO	FC	K	FO	FC	K	FO	FC	K	FO	FC	K	FO	FC	K	FO	FC

(Table 3 consists of a large, densely printed grid of observed and calculated structure factor values organized in multiple column groups, each introduced by H,L= index headers. The reproduction quality is too low to transcribe every numeric entry reliably.)
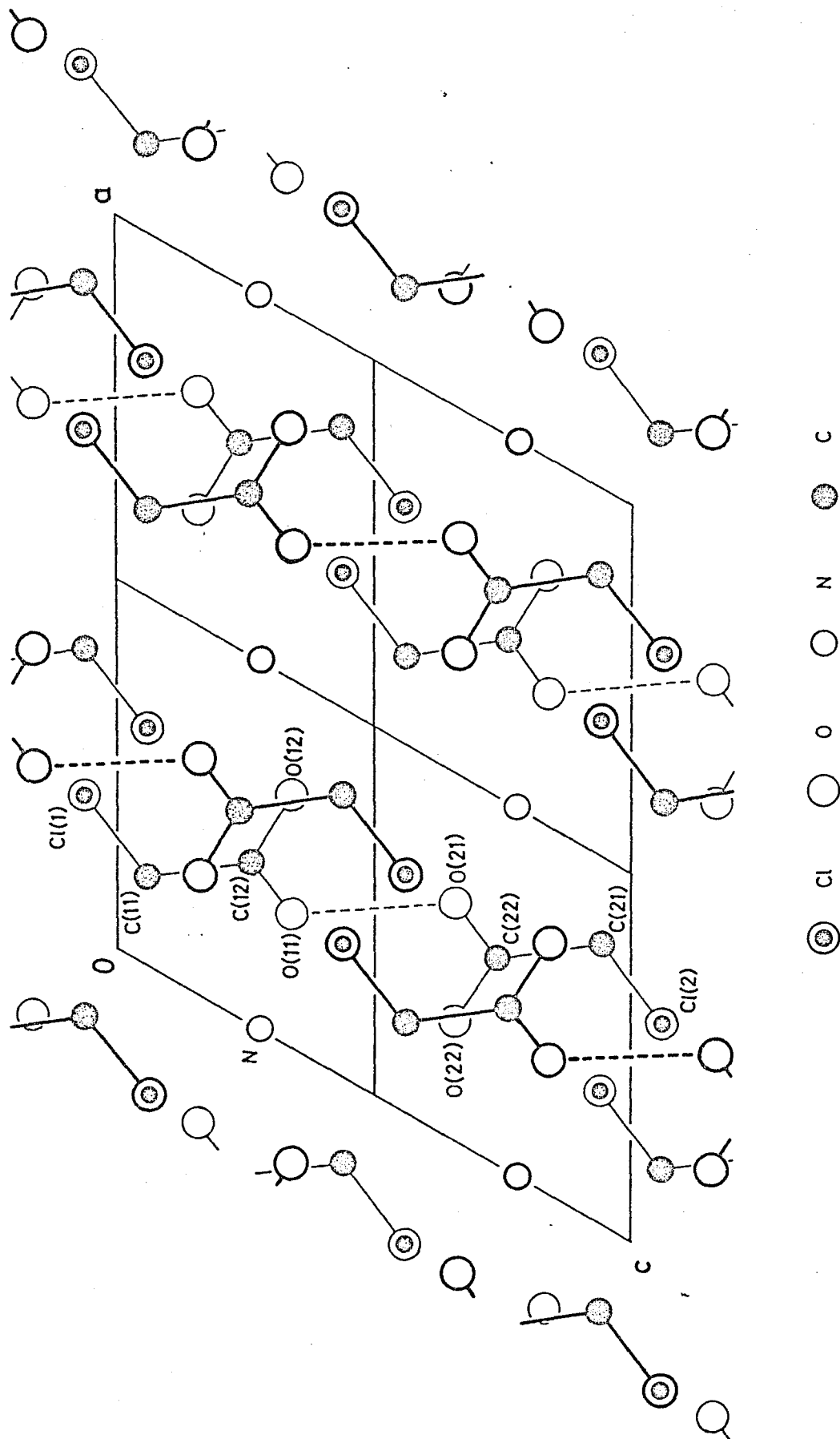
Fig. 2. The structure viewed along the b axis. The OHO hydrogen bonds are shown by broken lines.

numbering for the para- and the ferroelectric phase is listed in Table 4. The interatomic distances and angles are shown in Table 5 and Fig.3. Those obtained at room temperature are also given for comparison in Table 5.

Chloroacetate dimer

The carboxyl group and the α-carbon atom in each chloroacetate radical are approximately coplanar. The least-squares plane of the two carbon and two oxygen atoms of CA(1) is represented by the equation

$$-0.5892 \; X + 0.7746 \; Y + 0.2298 \; Z = 2.4820,$$

where the direction cosines are referred to the orthogonal axes a, b and c*, and X, Y and Z are expressed in $\overset{\circ}{A}$. The deviations of atoms from the plane are: O(11) -0.006, O(12) -0.006, C(11) -0.005, C(12) 0.017 $\overset{\circ}{A}$. The Cl(1) atom lies -0.131 $\overset{\circ}{A}$ out of the plane. The equation of the best plane of the two carbon and two oxygen atoms of CA(2) is given by

$$-0.6274 \; X + 0.7487 \; Y + 0.2142 \; Z = 2.6646,$$

and the deviations of atoms from the plane are: O(21) 0.003, O(22) 0.003, C(21) 0.002, C(22) -0.008 $\overset{\circ}{A}$. The Cl(2) atom lies 0.301 $\overset{\circ}{A}$ out of the plane.

The conformation of the chloroacetate dimer in the ferroelectric phase shows no definite change as compared with that in the paraelectric phase, including a very short hydrogen-bond distance of 2.457(16) $\overset{\circ}{A}$. If in the ferroelectric phase one of the two chloroacetate radicals were in the form of carboxylate (-COO⁻, fully ionized)

Table 4.   Correspondence of numbering of atoms in the
para- and ferroelectric phase.

paraelectric phase	$\longleftrightarrow$	ferroelectric phase
Cℓ		Cℓ(1), Cℓ(2)
O(1)		O(11), O(21)
O(2)		O(12), O(22)
N		N
C(1)		C(11), C(21)
C(2)		C(12), C(22)

Table 5.   Interatomic distances and bond angles at 80°K and at room temperature with their standard deviations

	80°K	R.T. (Å)
C(11) – Cℓ(1)	1.742(21)	1.768(4)
C(11) – C(12)	1.444(19)	1.506(4)
C(12) – O(11)	1.272(20)	1.278(4)
C(12) – O(12)	1.249(16)	1.225(3)
C(21) – Cℓ(2)	1.833(20)	
C(21) – C(22)	1.589(19)	
C(22) – O(21)	1.279(23)	
C(22) – O(22)	1.196(17)	
O(11)...O(21)	2.457(16)	2.432(5)
N^{iii} ... O(11)	2.876(17)	2.926(4)
N^{iv} ... O(12)	2.771(20)	2.880(3)
N ... O(12)	3.369(19)	3.148(3)
N^{iv} ... O(21)	2.929(17)	
N^{ii} ... O(22)	2.915(21)	
N ... O(22)	2.923(17)	

	80°K	R. T.
Cℓ(1) – C(11) – C(12)	114.9(1.1)	113.4(2)
C(11) – C(12) – O(11)	112.7(1.2)	111.4(2)
C(11) – C(12) – O(12)	125.0(1.5)	123.2(3)
O(11) – C(12) – O(12)	122.2(1.2)	125.4(3)
Cℓ(2) – C(21) – C(22)	109.3(1.1)	
C(21) – C(22) – O(21)	108.4(1.2)	
C(21) – C(22) – O(22)	122.2(1.5)	
O(21) – C(22) – O(22)	129.4(1.3)	
C(12) – O(11)...O(21)	112.5(8)	114.8(3)
C(22) – O(21)...O(11)	113.9(8)	

Superscripts refer to atoms at :

i)   x,   y,   z   iii) 1/2+x, 1/2+y, z

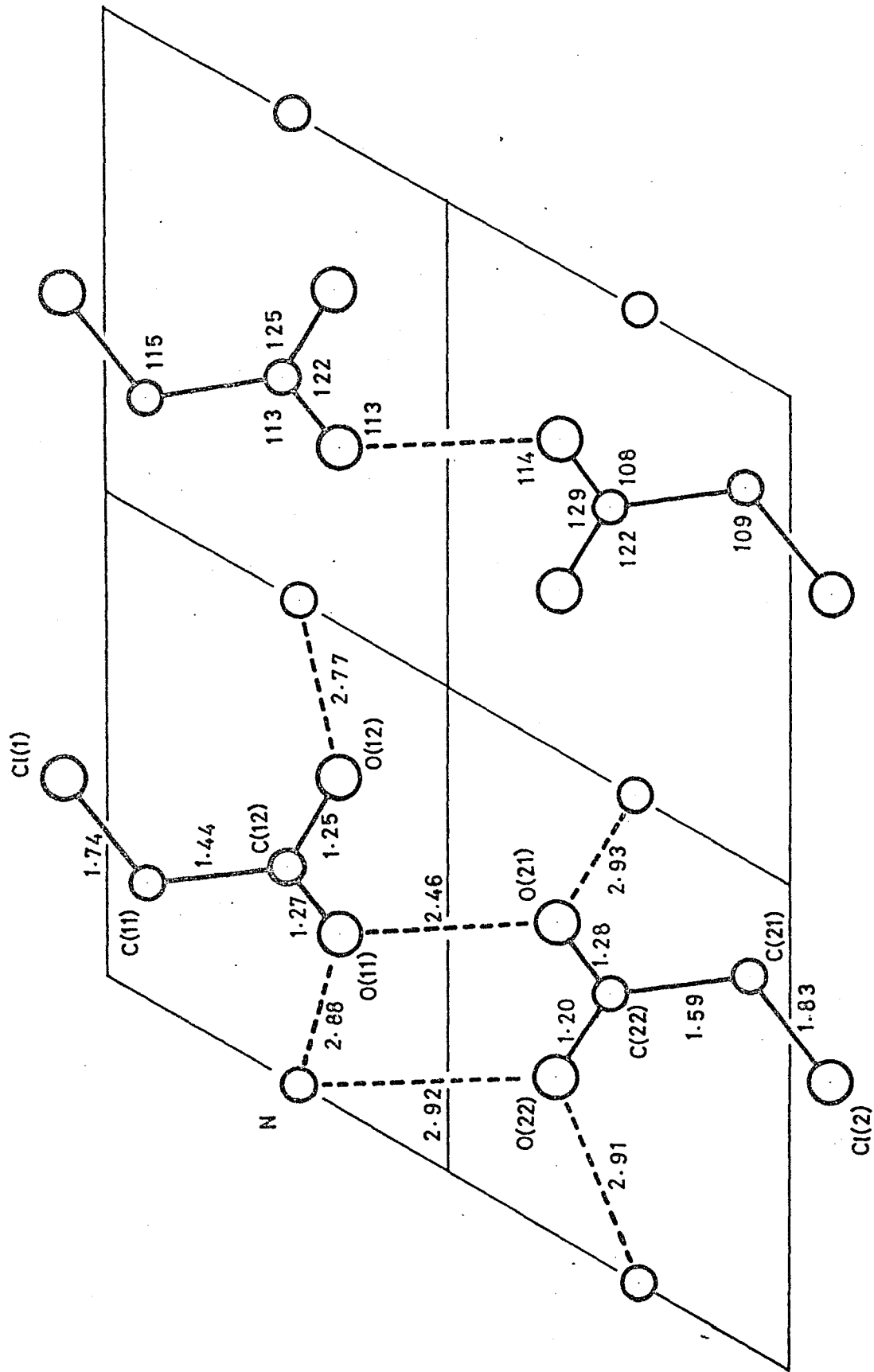ii) x, -y, 1/2+z   iv) 1/2+x, 1/2-y, 1/2+z

Fig. 3. The interatomic distances (Å) and angles (°) for structure at 80 K.

and the other in the form of carboxyl (-COOH, neutral),

the following tendency would be expected: in a carboxylate

group the two C-O bond-lengths and two C-C-O angles are

equal, whereas they differ in a carboxyl.[12] Moreover,

the length of the OHO hydrogen bond linking the two

radicals should show a definite increase[13] as compared

with that of the room-temperature structure, in which the

potential of the hydrogen atom was thought to be of the

single-minimum type.[1] The bond lengths and angles of

CA(1) and CA(2), however, do not show such a systematic

tendency (Fig.3). The length of the OHO hydrogen bond,

2.457(16) Å is still close to 2.432(5) Å of the room-

temperature value and to 2.445 Å which is the mean of

six most precise values for Type-A acid salts

(Table 6 in Chap.II). Judging from the results of the

present analysis, the chloroacetate dimer at 80° K seems

to retain still the same character as that found at room

temperature, i.e., a character intermediate between fully

ionized and neutral.

Ammonium ion

The nitrogen atom of ammonium ion is displaced

0.240 Å along the c axis from its position on the two-fold

axis which exists in the paraelectric phase. This shift

results in a considerable change in interatomic distances

between the nitrogen atom and the oxygen atoms of

CA(1) and CA(2) surrounding the nitrogen atom, as

compared with the room-temperature structure. In particluar, the following variations in the interatomic distances are noted: an increase of 0.221 $\overset{\circ}{A}$ in $N^{iv}...O(12)$, and a decrease of 0.225 $\overset{\circ}{A}$ in $N...O(22)$ and a decrease of 0.109 $\overset{\circ}{A}$ in $N^{iii}...O(12)$ (see Table 5).

III.5. On the ferroelectric phase transition

The acidic hydrogen atom or the ammonium ion is one of the most commonly found constituents of hydrogen-bonded ferroelectrics and is said to play an important role in the phase transition such as KH_2PO_4 and $(NH_4)_2SO_4$. One of the structural features of ferroelectric $NH_4H(ClCH_2COO)_2$ is that the asymmetric unit contains only one acid hydrogen atom and one ammonium ion. Thus the mechanism of the phase transition of $NH_4H(ClCH_2COO)_2$ should be simpler than the cases which asymmetric unit contains more than one of these ions, e.g. $(NH_4)_2SO_4$ and NH_4HSO_4, if these constituents solely play the crucial role. The special attention is paid to the OHO bond and the ammonium ion below.

The OHO bond

It has been concluded from the structure analysis at room temperature that the shape of the hydrogen atom in the OHO bond connecting two chloroacetate residues is

effectively of a single-minimum type in the paraelectric

phase. This result necessarily leads to the conclusion

that the acidic hydrogen atom does not drive the phase

transition, i.e. cannot be the trigger, in contrast to

the hydrogen atom in a double-minimum potential well.

This is also supported from the result that the

hydrogen-bond length remains still short at 80 K

(2.457(16) $\overset{\circ}{A}$) and falls in the range of other Type A

acid salts within the accuracy of the present analysis.

Chihara and coworkers[3-6] have extensively studied

the ferroelectric phase transtion in $NH_4H(ClCH_2COO)_2$

and $ND_4D(ClCH_2COO)_2$ by various experimental technique.

Chihara, Inaba, Nakamura and Yamamoto measured

temperature dependence of the ^{35}Cl nuclear quadrupole

resonance frequencies in $NH_4H(ClCH_2COO)_2$ and

$ND_4D(ClCH_2COO)_2$ and determined principal values of the

electric field gradient tensors at Cl sites for two

phases of H salts.[3] It was found that a single

resonance line in the high temperature paraelectric

phase splits into a pair of lines, whose separation is

proportional to the spontaneous polarization. Next

isotope effects were found; The transition temperature

rises by 11 K, the ratio of the splitting V_D'/V_H' was

2.17, and the ratio of the splitting in the C-Cl

stretching frequency in infrared spectra Δ_D/Δ_H was

2.16.[4] Two possible mechanisms of the ferroelectric

phase transition, continuous displacive type and

order-disorder type, are examined, but definite conclusion could not be drawn because both mechanisms account equally for the experimental results. Successively the ^{35}Cl nuclear quadrupole frequencies in the ferroelectric phase and the relaxation times T_1 were measured in two phases by Chihara, Nakamura and Okuma.[5] T_1 decreases steeply in the vicinity of the transition temperature, the anomalous part of which was attributed to the critical fluctuations of the polarization. A large dip of T_1 in the critical region was analyzed by two models as well, i.e. order-disorder model and displacive model. The order-disorder type of mechanism can explain the T_1 data of the paraelectric phase, but cannot explain the different temperature dependence of T_1 of two lines, while displacive type mechanism gives a reasonable description of the T_1 anomaly both in the ferro- and paraelectric phase. The difficulty in order-disorder model also emerged from the heat capacity measurement in $NH_4H(ClCH_2COO)_2$ and $ND_4D(ClCH_2COO)_2$ by Chihara and Inaba[6] in which the observed entropy 2.90 $JK^{-1}mol^{-1}$ is only half the magnitude predicted by a simple order-disorder model, $Rln\ 2$ or 5.76 $JK^{-1}mol^{-1}$. It was also pointed out from the heat capacity as well as differential analysis[3] that the transitions are of second or higher order in contrast to our suggestion.[14]

Temperature dependencies of infrared and Raman spectra in $NH_4H(ClCH_2COO)_2$ and $ND_4D(ClCH_2COO)_2$ were

reported by Chihara, Nakamura and Inaba.[4] No well defined

soft mode was found in Raman spectrum, but they report weak

peaks aroun 200 cm^{-1} which depend on temperature. The broad

and intense O-H (900 cm^{-1}) and O-D (850 cm^{-1}) stretching

bands was also observed in the infrared spectrum, which is

consistent with our observation (II.5., Fig.6). The

significant temperature dependence of the band width and

intensity was observed in the OCO in-plane bending mode.

Hadži and Orel[15] carried out an infrared absorption

study of $NH_4H(ClCH_2COO)_2$ at 293 K and 93 K, and found

that no significant change of bands associated with the

OHO and carboxyl group vibration occurs. They concluded

that the short hydrogen bond is not directly involved in

the constituents which play the major role in the

ferroelectric phase transition. As a whole, as for the

mechanism of the ferroelectric phase transition in

$NH_4H(ClCH_2COO)_2$ there are no serious contradictions

between the conclusion drawn from our present structure

analyses and those from other experimental techniques,

i.e. the ^{35}Cl nuclear quadrupole resonance frequency and

relaxation time, heat capacity measurement, and infrared

and Raman spectrum, in the point that order-disorder

mechanism of the acidic hydrogen atom is ruled out.

The ammonium ion

With reference to the ammonium ion, it seems

necessary to begin by investigating whether the electron

density of the nitrogen atom at room temperature can be

explained by a superposition of two stable sites. For this

purpose, two electron-density maps of the nitrogen atom

are compared in Fig.4. Fig.4(a) is the contour map

obtained from the photographic data at room temperature.[1]

Fig.4(b) is the calculated map,

$\rho'(x,y,z) = \frac{1}{2}\left\{\rho(x,y,z) + \rho(-x,y,\frac{1}{2}-z)\right\}$, from the electron

density $\rho(x,y,z)$ of the nitrogen atom at 80° K,

assuming a disorder distribution satisfying the presence

of the twofold axis. This implies that the displacement

of the nitrogen atom from the twofold axis is independent

of temperature, i.e., a pure order-disorder. The shape

of the contours in the two maps should be the same if the

above assumption holds. The shape of the superposed

contours, however, is slightly elongated along the c*

axis in comparison with that at room temperature.

We now consider the temperature factors. The

component of the displacement of the nitrogen atom along

the c and c* axes from the twofold axis is denoted by

ΔR_c and ΔR_{c*} respectively, where ΔR_{c*} is expressed by

$\Delta R_{c*} = \Delta R_c \cos(\beta - 90°)$. Assuming a pure order-disorder,

the r.m.s. amplitude of the thermal vibration obtained

from the results at room temperature, U^d_{c*}, is expressed

by $U^d_{c*} = \Delta R_{c*} + U^o_{c*}$, where U^o_{c*} is the r.m.s. amplitude

which would be expected if the nitrogen atom were ordered.

This equation can be applied at 80° K as well, and U^o_{c*}

can be obtained directly from the present analysis.

If the above model is correct, U^d_{c*} is expected to be
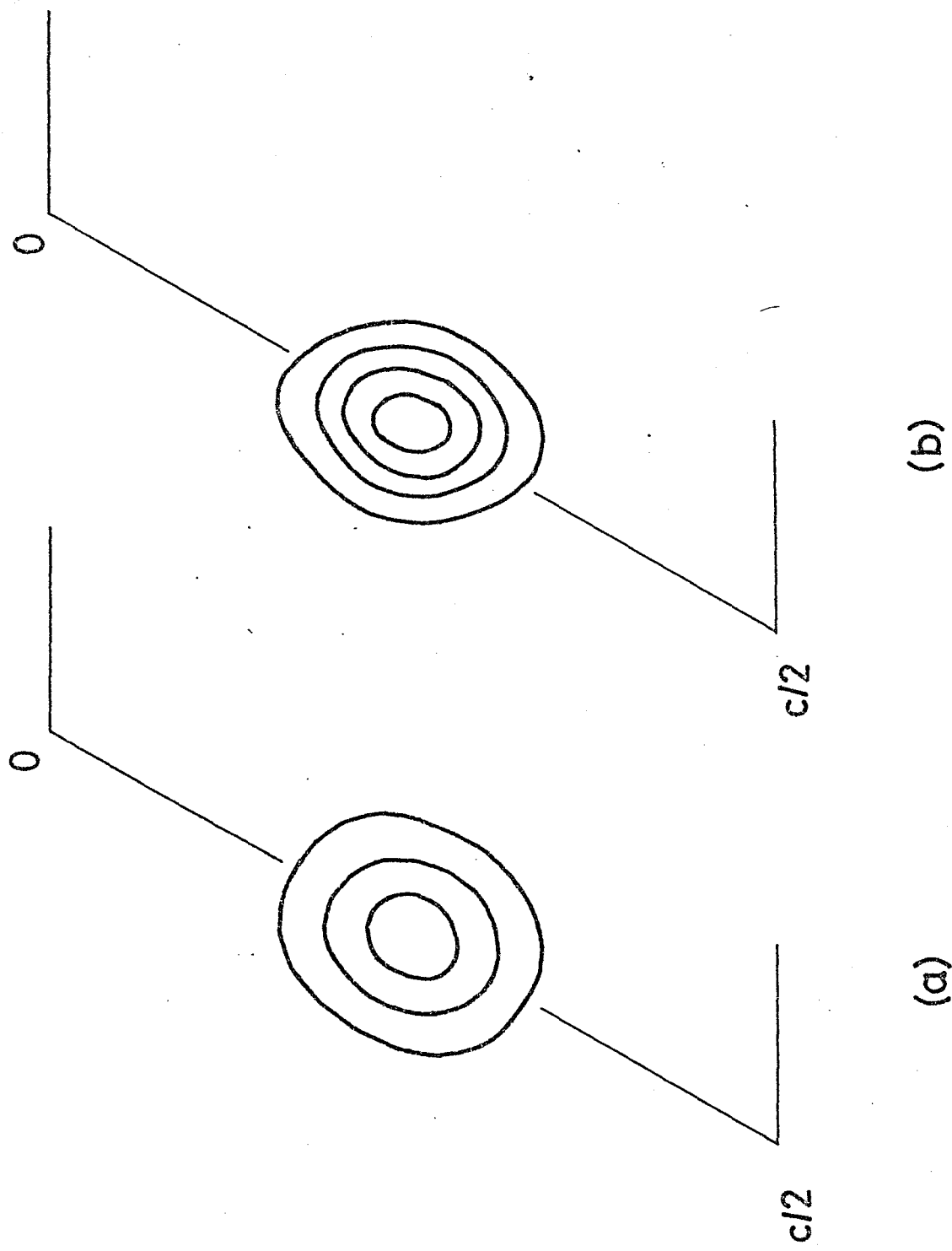
Fig. 4. The electron-density maps of the nitrogen atom viewed along the b axis at room temperature (a) and the calculated average one at 80 K (b). See text for details.

greater at room temperature than at 80° K. However, at room temperature, U_{c*}^d obtained from B_{33} was 0.296(8) $\overset{\circ}{A}$ and 0.280(4) $\overset{\circ}{A}$ from the photographic and the counter data respectively, whereas at 80° K, U_{c*}^d obtained through B was 0.344(22) $\overset{\circ}{A}$. Judging from the shape of the contours in Fourier maps (Fig.4) and the r.m.s. amplitude of thermal vibrations, a pure order-disorder mechanism of the nitrogen atom of the ammonium ion may also be excluded from taking into consideration.

Chihara, Inaba, Nakamura and Yamamoto[3] examined a possibility that some motion of the ammonium ion play a role in the phase transition by proton magnetic resonance. However, it was ruled out since no discontinuous change was found at the transition temperature in the line width as well as in the spin-lattice relaxation time. This is also supported by the result that the spin-spin relaxation time T_2 shows only a shallow dip in the neighbourhood of the transition temperature, which is closely associated with the motion of the ammonium ion. Thus there is also no discrepancy between the conclusion from our structural aspect and those from the proton magnetic resonance and the ^{35}Cl nuclear quadrupole resonance studies.

Polarization reversal

Spontaneous polarization is switched by a change of CA(1)⟷CA(2). The displacements of each atom during

switching are listed in Table 6. It is seen that the displacement of the nitrogen atom is fairly large as compared with those of the other atoms. The value of the spontaneous polarization at 77° K is 0.18 μC.cm^{-2} along [102].[14] This is smaller by one or two order of magnitude compared with well-known ferroelectrics such as $BaTiO_3$, SbSI, $NaNO_2$, KH_2PO_4 and $(NH_2CH_2COOH)_3 \cdot H_2SO_4$.[16]

One of the future problems in $NH_4H(ClCH_2COO)_2$ will be the study of origin of the ferroelectric phase transition based upon more detailed knowledge of temperature variation of the atomic configuration and the atomic motion. Chihara, Inaba and Okuma[5] suggest that the ferroelectric transition in $NH_4H(ClCH_2COO)_2$ is one of the displacive type where one of the transverse optic modes associated with the proton motion couples anharmonically with other normal mode including ammonium ions, and this strong anharmonicity comes from the dipolar coupling between the ammonium ions and protons via the chloroacetate anions. Recently Chihara and Inaba[6] pointed out a possibility of an improper ferroelectric, which is compatible with a small value of Curie-Weiss constant (44).[14]

The other problem is what position the characteristic of the hydrogen bond (symmetric, 2.432 Å) and the deuteration effect in transition temperature (11 K) occupy

Table 6.   Displacements of atoms during switching (Å)

	Δa	Δb	Δc	Total Δ
Cℓ(1)⟷Cℓ(2)	0.015	0.082	0.038	0.089(5)
O(11)⟷O(21)	0.166	0.030	0.219	0.202(14)
O(12)⟷O(22)	0.012	0.143	0.004	0.167(14)
N ⟷ N	0.001	——	0.479	0.479(24)
C(11)⟷C(21)	0.093	0.044	0.039	0.125(29)
C(12)⟷C(22)	0.119	0.054	0.189	0.175(18)

in general hydrogen bonds and general hydrogen-bonded ferroelectrics and whether this problem can be explained reasonably, which are discussed in next chapter.

References

1) M. Ichikawa: Acta Cryst. B28 (1972) 755.

2) M. Ichikawa: Acta Cryst. B30 (1974) 651.

3) H. Chihara, A. Inaba, N. Nakamura and T. Yamamoto: J. Phys. Soc. Japan 35 (1973) 1480.

4) H. Chihara, N. Nakamura and A. Inaba: J. Phys. Soc. Japan 36 (1974) 1710.

5) H. Chihara, N. Nakamura and H. Okuma: J. Phys. Soc. Japan 37 (1974) 1385.

6) H. Chihara and A. Inaba: J. Phys. Soc. Japan 40 (1976) 1383.

7) International Tables for X-ray Crystallography (Kynoch Press, Birmingham, 1959 and 1962) Vol.II and Vol.III.

8) D. C. Phillips: Acta Cryst. 9 (1956) 819.

9) J. S. Rollett and R. A. Sparks: Acta Cryst. 13 (1960) 273.

10) A. J. C. Wilson: Acta Cryst. 2 (1949) 378.

11) UNICS Universal Crystallographic Computing System, ed. T. Sakurai (Crystallographic Society of Japan, 1967).

12) T. Hahn: Z. Krist. 109 (1957) 438.

13) M. Ichikawa: Submitted to Acta Cryst. B (1978).

14) M. Ichikawa and T. Mitsui: Phys. Rev. 152 (1966) 495.

15) D. Hadži and B. Orel: J. mol. Struct. 18 (1973) 227.

16) T. Mitsui: Landolt-Börnstein. Numerical Data and

Functional Relationships in Science and Technology

ed. K.-H. Hellwege and A. M. Hellwege

(Springer, Berlin, 1969) New Series III/3.

Ferro- and Antiferroelectric Substances.

Chapter IV.   The O-H vs O...O Distance Correlation and

the Geometric Isotope Effect in OHO Hydrogen Bonds

IV. 1.   Introduction

It is well known that there exist some correlations

between H-bond parameters, since in 1955 Nakamoto,

Margoshes and Rundle[1] have pointed out that the O-H bond

length decreases with increasing the O...O distance.[2-4]

However, it seems that the details of the correlation remain

unsettled in the short and very short regions of O...O

length, especially with respect to the dependence on the

O...O distance, surroundings and symmetry of the

hydrogen bond system.

The other important phenomenon for the understanding

of the nature of hydrogen bonding is a geometric

isotope effect. Since the works by Ubbelohde and

coworkers[5] it seems to have been established that an

expansion of the hydrogen bond length is observed when

deuterium is substituted for hydrogen in crystals.

However, there is still uncertainty about the following

respects: whether the size of the geometric isotope

effect is a function of the hydrogen bond length, and

how large is its maximum, and what are the factors

influencing the isotope effect. This mainly seems to

result from that the magnitude of the effect is as small as $\sim 10^{-2}$ Å. Thus, the results obtained from indirect information of lattice-spacing measurement, which assumes that any changes from isotopic substitution are confined to the hydrogen-bond system, may not be regarded as the real effect with sufficient reliability. Even with recent direct structure analysis the accuracy of $\sim 10^{-3}$ Å in hydrogen-bond length, which is desirable in discussing the geometric isotope effect, is not always attained. However, since the accuracy of crystal structure determinations has greatly increased, particularly in the past ten years, many hundred accurate structures have been published, thus giving us the opportunity to reinvestigate the correlation between structural data in detail.

On the other hand, it is well known that some of hydrogen-bonded crystals, which undergo ferro-, antiferroelectrics, or other type of phase transition, exhibit an anomalous isotope effect. For example, in a series of KH_2PO_4-type crystals, the transition temperature Tc rises by a maximum of about 100 K on deuteration. The role of the hydrogen bond in the phase transition and the origin of the isotope effect in these crystals seems to be not yet fully understood. The phase-transition mechanism and the isotope effect in hydrogen-bonded ferro-, antiferroelectrics, and other materials are expected to be closely associated

with the characteristic of the hydrogen bond. To obtain
further knowledge on the nature of the hydrogen bond
seems indispensable for deeper understanding of these
problems in hydrogen-bonded crystals.

The purpose of this chapter is to establish the
correlation between the hydrogen-bond parameters and the
geometric isotope effect, and to discuss the relation
of the structural isotope effect of the symmetric
hydrogen bond with the anomalous increase in Tc by using
these correlation curves as an empirical basis.[6]
Brown[7] discussed the geometry of OHO bonds, mainly in
the medium and long regions, in connection with the bond
valence. Olovsson and Jönsson[8] has recently surveyed
X-ray and neutron crystal structural data and referred
to the correlation between hydrogen-bond parameters
and the geometric isotope effect independently.
Hence, the results on the O-H vs O...O correlation and
the geometric isotope effect are described briefly and
these application and discussion are stressed.

IV.2. Data collection

Crystal structure data obtained by X-ray and
neutron diffraction have been taken from the literature.
A part of the literature used was retrieved with
TOOL-IR system.[9] Hydrogen-bond parameters were

recaluculated with UNICS[10] if they and their estimated

standard deviations were not specified in the literature.

The data were used for a discussion of correlations between

hydrogen-bond parameters only if the e.s.d's of all the

relevant length were equal to or less than 0.010 Å, the

O...O distance was less than 3 Å, and O-H...O angle

larger than 150°. The data used consisted of 227 bonds

and 79 compounds, including the data of Brown[7] and

Olovsson and Jönsson.[8] A list of the data were given in

Appendix. The values not corrected for thermal motion

were used. If two or more studies are made on the same

compound, the data with the smaller e.s.d's were adopted.

For discussion of the geometric isotope effect,

the threshold value of a combined standard deviation of

0.005 Å was taken; the combined standard deviation is

defined as $\sigma = (\sigma_H^2 + \sigma_D^2)^{\frac{1}{2}}$, where σ_H and σ_D are

e.s.d's of O...O distance in the hydrogen and

corresponding deuterium compound. The remaining data

include those from X-ray as well as neutron diffraction.

If both were available, they are both listed (Table 1),

but the data with the smallest e.s.d's are plotted

(Fig.2), as any systematic difference could not be

found within experimental error.

IV.3. The symmetric hydrogen-bond

For the following discussion, first the term 'symmetric hydrogen bond' should be referred to because its implication seems equivocal among literature, as pointed out by olovsson and Jönsson.[8] As far as the author is aware one is used with respect to the type of the hydrogen-atom potential curve: (i) a hydrogen bond is said to be symmetric when the potential is of single-minimum type, or when the potential is of single-minimum type with a minimum at the mid-point of two oxygen atoms, whether there is crystallographic equivalence between a donor and an acceptor atom or not. The second refers to crystallographic symmetry: (ii) a hydrogen bond is said to be symmetric if the donor and acceptor atom are crystallographically equivalent, regardless of the type of potential curve.

Speakman and coworkers[4,11] classified acid salt of carboxylic acids using criterion (ii). Catti and Ferraris[12,13] took the position of (i) and, furthermore, introduced the word 'symmetry restricted' (SR) for (ii). In this paper the description 'symmetric' is confined to (ii), the term 'single' of 'double minimum' being added if necessary to describe the bonding situation. It is possible to express all probable types of hydrogen bond by using these terms. The terms 'symmetric' and 'centered' proposed by Olovsson and Jönsson[8] are mostly consistent with our standpoint if 'symmetric' is restricted within (ii), and 'centered' is replaced by 'single-minimum'.

IV.4. The Correlation between O-H vs O...O distance

A correlation diagram of O-H vs O...O distance is
shown in Fig.1.

Symmetric bond

In a region of R(O...O) < 2.5 Å, i.e. very short
hydrogen bonds in Speakman's classification,[4,11]
symmetric bonds are continuously distributed 2.419 to
2.468 Å. In this region the conclusion drawn from an
thermal ellipsoid analysis agrees with the theory that
the potential curve is effectively of single-minimum
type; it is of single-minimum, or broad and anharmonic or
if a barrier exists it is small compared with the ground
state vibrational level.[12,30] It should be stressed
that symmetric hydrogen bonds are not restricted to the
very short region, but can be found also at least up to
2.6 Å, though the bonding situation may be different from
those in the very short region. Examples are a series of
KH_2PO_4-type crystals[3] (around 2.5 Å), $KH_3(SeO_3)_2$
(2.566 Å),[13] $NaH_3(SeO_3)_2$ (2.602 Å)[14], and the number
will increase further taking into consideration much
amount of X-ray data. Lehmann and Larsen[13] performed a
least-squares refinement of symmetric hydrogen bond
(2.566 Å) of $KH_3(SeO_3)_2$ with two models, i.e. one that
distributes the H atom statistically on two side of a
special position (disordered model) and one that locates
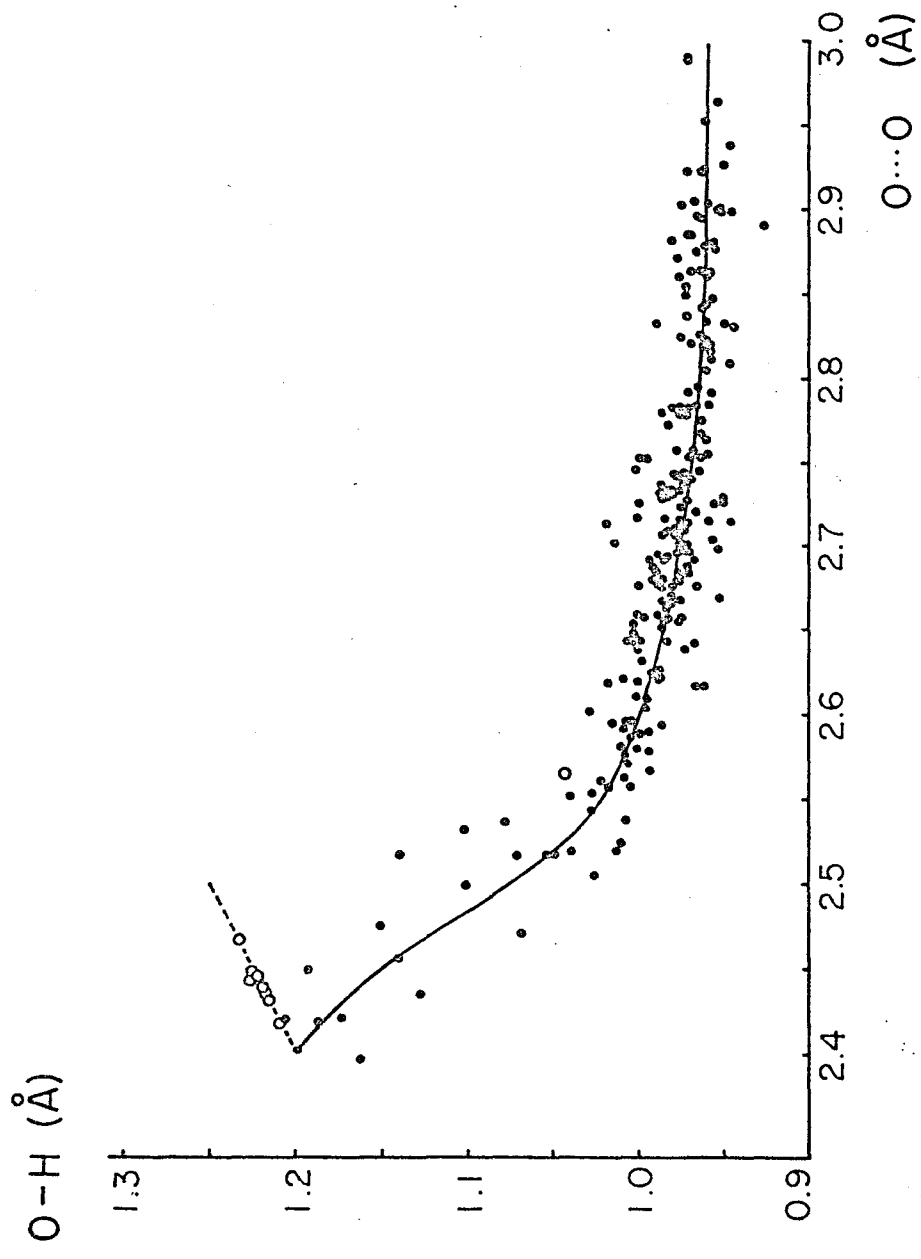
Fig. 1. A diagram of correlation between O-H and O...O distance in OHO hydrogen bonds. Open circle : symmetric bond ; filled circle : asymmetric bond.

it in a special position (ordered model). On the basis
of the Hamilton test on the weighted R factor ratio they
reached the conclusion that the disordered description
is significantly better than the ordered one. It is
worth mentioning that the O-H length refined with a
disordered model falls on the correlation line of the
asymmetric bonds. It will be worthwhile to note here
that the analysis of the thermal motion is done within the
framework of a harmonic approximation and therefore the
better fit of the disordered model indicates the potential
curve to be anharmonic, but not necessarily mean it to be
of real double-minimum type with the meaning that the
barrier is higher than the ground state vibraional level,
as discussed in II.5. Kaplan, Kay and Morosin[14]
reported for the symmetric bond of 2.602 $\overset{o}{A}$ in $NaH_3(SeO_3)_2$
that the difference synthesis indicates disorder.

It can be concluded that symmetric hydrogen bonds are
distributed continuously at least up to about 2.6 $\overset{o}{A}$, and
that the shape of the H atom potential curve seems to
vary continuously from single- to double-minimum type
with increasing O...O distance, retaining the symmetry
requirement (schematically as (e)$\rightarrow$(d)$\rightarrow$(c) in Fig.1 of
Chap. I). Because of this situation regarding symmetric bonds
it appears extremely difficult to distinguish between single
and double-minimum for symmetric hydrogen bonds around
2.5 $\overset{o}{A}$.

Asymmetric bond

Asymmetric hydrogen bonds are distributed over all region. As an average the O-H length increases gradually in a medium and a long region with decreasing the O...O, and increases more rapidly in the region less than about 2.55 $\overset{\circ}{A}$ (schematically as (a)$\rightarrow$(b)$\rightarrow$(f) in Fig.1 of Chap.I). The average correlation curve does not jump discontinuously or approach very rapidly the 'symmetric' straight line at a particular O...O length, but appears to coincide with it at the shortest limit near 2.4 $\overset{\circ}{A}$.

The deviation of each point from the average correlation curve becomes large as the O...O distance is less than about 2.55 $\overset{\circ}{A}$; In the longer-bond region more than 90 % of the points are within 0.02 $\overset{\circ}{A}$ of the smoothed curve, whereas in the shorter-bond region this figure is only 40 %. This seems to reflect that the potential curve become flat when the O...O distance is shorter than 2.55 $\overset{\circ}{A}$ and the equilibrium position of the H atom shifts from the average according to the characteristic of the differing environment of the hydrogen bond.

IV.5. Geometric isotope effect

The difference in the O...O distance caused by substituting deuterium for hydrogen, ΔR, is called the geometric isotope effect in this paper;

$\Delta R = R(O...O)_D - R(O...O)_H$ where $R(O...O)_D$ and $R(O...O)_H$ denote the hydrogen and corresponding deuterium bond length. The $(O...O)_H$ and $(O...O)_D$ notation are used only if it is necessary to distinguish between them, otherwise $O...O$ is used. The relevant data are listed in Table 1 and ΔR is plotted against $O...O$ distance in Fig.2.

Fig.2 shows that there exists a correlation between ΔR and $R(O...O)_H$: the positive isotope effect, i.e. expansion can be seen in the $O...O$ region of about 2.44-2.64 Å, with a maximum value of 0.027 Å. This corresponds to the correlation between the isotope ratio of antisymmetric OH stretching frequency $\nu OH/\nu OD$ and $R(O...O)_H$ by Novak.[15] ΔR appears to increase and decrease rapidly near 2.44 and 2.64 Å respectively. For the region shorter than 2.44 Å and longer than 2.64 Å, no isotope effect can be recognized except for the case of $\alpha-(COOH)_2 \cdot 2H_2O$[16] discussed below. These results are compatible with theoretical prediction by Rundle[17] and Singh and Wood.[18] Further definite conclusion cannot be drawn at present for lack of number of data.

It may be worth while to consider here what factors smear the correlation, since there seems to be room for argument as to whether a correlation between ΔR and $R(O...O)_H$ is present or not. Finholt and Williams[19] state that no correlation seems to exist. Thomas[20] and Olovsson and Jönsson[8] considered that in a crystal with more than one species of hydrogen bond only short bonds

Table 1. Geometric isotope effect

The O...O distance is the value at room temperature.

X and N denote X-ray and neutron diffraction method

respectively.

Compound & references		O...O (Å)	ΔR (Å)	D content	Method
Squaric acid	23	2.548(1)	0.027(1)		X
		2.549(1)	0.024(1)		
$YH(C_2O_4)_2 \cdot 3H_2O$	24	2.440(3)	0.013(5)	0.884	N
		2.643(2)	-0.003(3)	0.918	
		2.680(2)	0.000(3)	0.913	
KH_2PO_4	25	2.496(1)	0.023(1)		X
$KHCO_3$	26	2.585(2)	0.022(3)		X
		2.587(1)	0.020(2)		N
$\alpha-(COOH)_2 \cdot 2H_2O$	16	2.512(1)	0.019(1)		X
		2.864(2)	0.016(3)		
		2.883(1)	0.024(1)		
		2.506(4)	0.018(4)		N
		2.864(5)	0.015(5)		
		2.881(4)	0.025(4)		
$KH_3(SeO_3)_2$	13	2.566(1)	0.014(2)	0.846	N
		2.602(2)	0.021(3)	0.871	
$LiHC_2O_4 \cdot H_2O$	20	2.490(1)	0.016(1)		X
		2.702(1)	-0.002(1)		
		2.777(1)	0.001(1)		
$N_2H_5HC_2O_4$	27	2.457(1)	0.009(2)		X

Table 1. (continued)

Compound & references		O...O (Å)	ΔR (Å)	D content	Method
$(H_5O_2^+)_2SO_4^{2-}$	28	2.431(3)	-0.005(4)		X
		2.664(2)	0.002(3)		
		2.655(2)	0.000(3)		
$NaHC_2O_4 \cdot H_2O$	29	2.571(2)	0.022(3)		X
		2.826(2)	0.000(3)		
		2.808(2)	0.001(3)		
$KH(CF_3COO)_2$	30	2.437(4)	0.000(5)	0.905	N
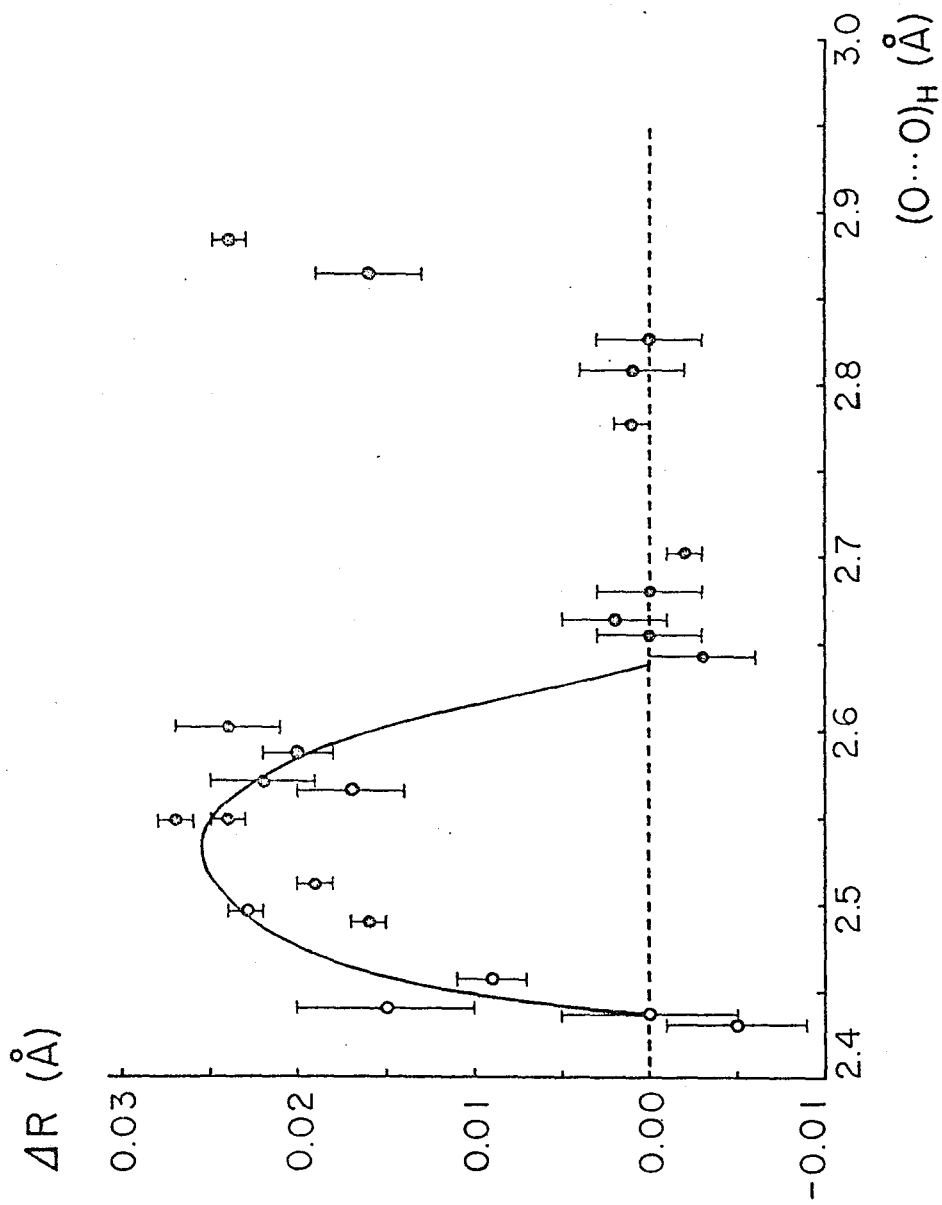
Fig. 2. The geometric isotope effect, ΔR, as a function of $(O\cdots O)_H$ length.

(up to 2.6 Å) exhibit the genuine isotope effect and long bonds do not, since changes in the latter are exerted by the influence of the structural rearrangement induced by the genuine isotope effect of the short bonds.

The following may be pointed out as possible factors smearing the correlation. (i) Insufficient accuracy. (ii) Incomplete deuteration. (iii) Direct coupling of the geometric isotope effect of an individual bond in a crystal involving with two or more species of hydrogen bond.

As the geometric isotope effect is of the order of $\sim 10^{-2}$ Å at most (Fig.2), high accuracy of structure determination is required. First it should be emphasized that collection only of accurate data revealed the correlation. Secondly, perfect deuteration can not be achieved in spite of many times of recrystallization in D_2O and precaution taken to prevent H_2O contamination.[19] From the average of the real deuterium contents (0.899) in the crystals quoted in Table 1 intended as perfectly deuterated, which were obtained from least-squares refinement of the deuterium scattering amplitude for neutrons, deuterated crystals are considered to involve usually about 10 % incompleteness.

The third respect is associated with the hydrogen-bond arrangement in a crystal. Deviation from the above general trend of the isotope effect can be recognized in $\alpha - (COOH)_2 \cdot 2H_2O$[16] and in crystalline $H_3O^+CH_3C_6H_4SO_3^-$

crystal; in the former the two longer bonds also show the

large positive effect as well as the short one,

whereas in the latter three short bonds in the region

expected to show the large isotope effect exhibit only

much smaller effect. However, the common feature of

hydrogen bond arrangement can be pointed out in two cases.

It may be denoted schematically as follows for

a) α-$(COOH)_2 \cdot 2H_2O$ and b) $H_3O^+ CH_3 C_6 H_4 SO_3^-$;

(a)   (b)
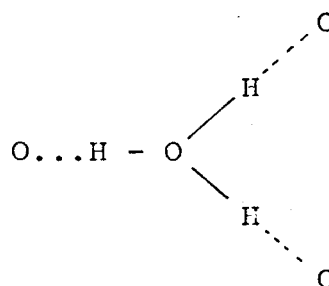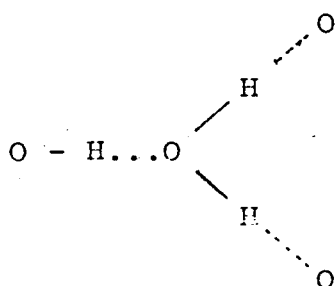
in two cases three H-bonds directly couple each other

through the central oxygen and each of them is

crystallographically independent. This situation seems

to make it difficult to obtain the genuine isotope

effect of the individual bond separately.

Strictly speaking, the geometric isotope effect

cannot be confined to hydrogen-bond system and necessarily

leads to the structural change of its neighbours.

The degree of coupling between hydrogen bonds may be

different from crystal to crystal. However, it may still

be possible that substitution of D for H does not result

in the rearrangement distributed throughout the structure,
if the hydrogen-bond systems are not directly coupled each
other. We believe that for long bonds the geometric
isotope effect is equally genuine as well as for short
bonds except some special cases as mentioned above.

IV.6. Symmetric bond and phase transition

Let's consider the structure of a linear symmetric
hydrogen bond on the basis of the assumption that the
potential curve of the symmetric bond can be expressed as
a superposition of the curves of two asymmetric bonds,
and the correlation curve between O-H and O...O
distance can be used as an empirical basis for the
equilibrium position of the H atom. This seems plausible
since the symmetric bonds exist continuously at least up
to about 2.6 Å and the values of O-H length refined with
a disordered model agree with those of the asymmetric bond.
Catti and Ferraris[21] discussed the disordered nature of
symmetric bonds in the very short region, which is
compatible with the present assumption. Then the distance
between two equilibrium positions of H atom, δ , is
written as

$$\delta = R(O...O) - 2R(O-H)$$

As shown in Fig.3, δ increases, with a maximum slope
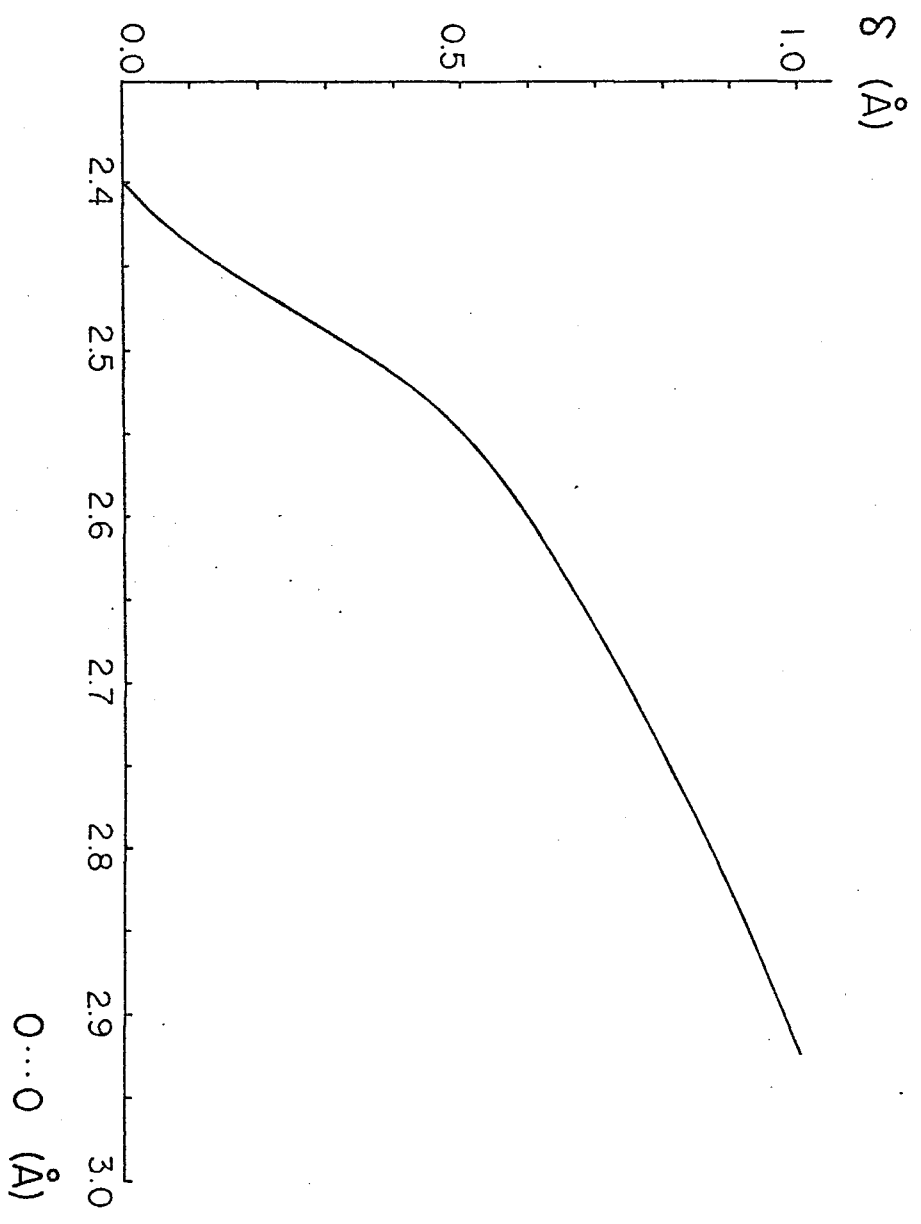
Fig. 3. The distance between two equilibrium positions in a symmetric hydrogen bond, δ , as a function of O...O length.

around 2.48 Å as the O...O distance increases, and
gradually approaches a straight line. It is noted here
that δ does not mean immediately the distance between
two minima in a double-minimum potential well since the
shape of the basic potential-energy surface and the
vibrational level are not known from diffraction data
alone.

If the O...O distance expands by an amount of ΔR
according to the ΔR vs $R(O...O)$ correlation curve when
a D atom is substituted for H, the O-D distance will be
equal to the O-H value corresponding to the length
$R(O...O)_H + \Delta R$ from the O-H vs $R(O...O)_H$ curve;
$R(O-D) = R(O-H) - \Delta R(O-H)$, where $\Delta R(O-H)$ denotes a
contraction of the O-H distance due to an expansion of
$R(O...O)$ by ΔR.   Then the distance between the two
equilibrium positions of the corresponding D bond is
expressed as

$$\delta_D = R(O...O)_D - 2R(O-D)$$

$$= \delta_H + 2\Delta R(O-H) + \Delta R,$$

where the subscript H and D are used only if it is necessary
to distinguish between the H and D bond.   This situation
is illustrated in Fig.4. The isotope effect of the
distance between two equilibrium positions $\delta_D - \delta_H$
consists of two terms: in the short-bond region where
the O-H length varies rapidly with O...O distance,
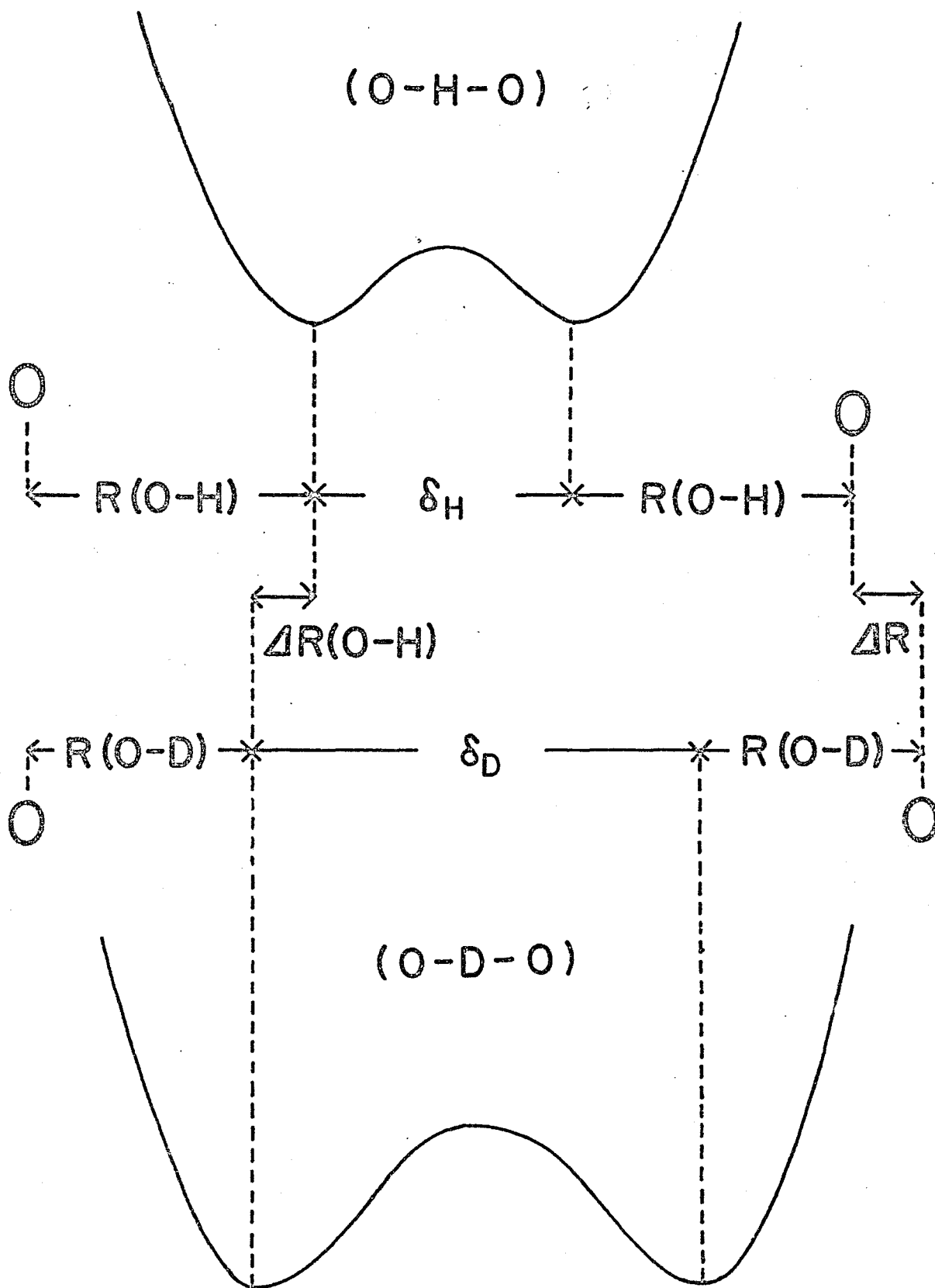
Fig. 4.   Schematic illustration of the geometric isotope

effect in a symmetric bond.

$2\Delta R(O-H)$ contributes mainly to the total $\delta_D - \delta_H$ and
amounts to about three times ΔR at maximum, whereas in
the long-bond region where O-H varies more slowly with
O...O, ΔR is the more dominant. With increasing
O...O $\delta_D - \delta_H$ increases rapidly and reaches its maximum
value around 2.49 Å and then decreases more slowly, as
shown in Fig.5. The functional behavior of δ_H and
$\delta_D - \delta_H$ should not be regarded as being fully established
at the present stage because it largely depends on the
accuracy of the correlation curve of R(O-H) vs R(O...O)
and ΔR vs R(O...O). However, it should be emphasized
that if ΔR itself is small, $\delta_D - \delta_H$ induced by ΔR
becomes four times as large as ΔR. The effect of ΔR
seems to have been overlooked or underestimated so far.[22]

The role of the hydrogen bond in hydrogen-bonded
crystals which exhibit ferroelectric, antiferroelectric
and other structural phase trnasition seems closely
associated with the characteristic of the hydrogen bond,
i.e. that of the potential curve. Therefore, an
anomalous isotope effect in physical quantities, such as
the transition temperature T_c is likely to be closely related
with difference between the features of the potential
curve of the hydrogen bond and its corresponding
deuterium bond; it may be reflected in the magnitude of
ΔR and $\delta_D - \delta_H$. A large shift of T_c may be expected
when the crystal has a symmetric hydrogen bond in a
paraelectric or high temperature phase, and its O...O
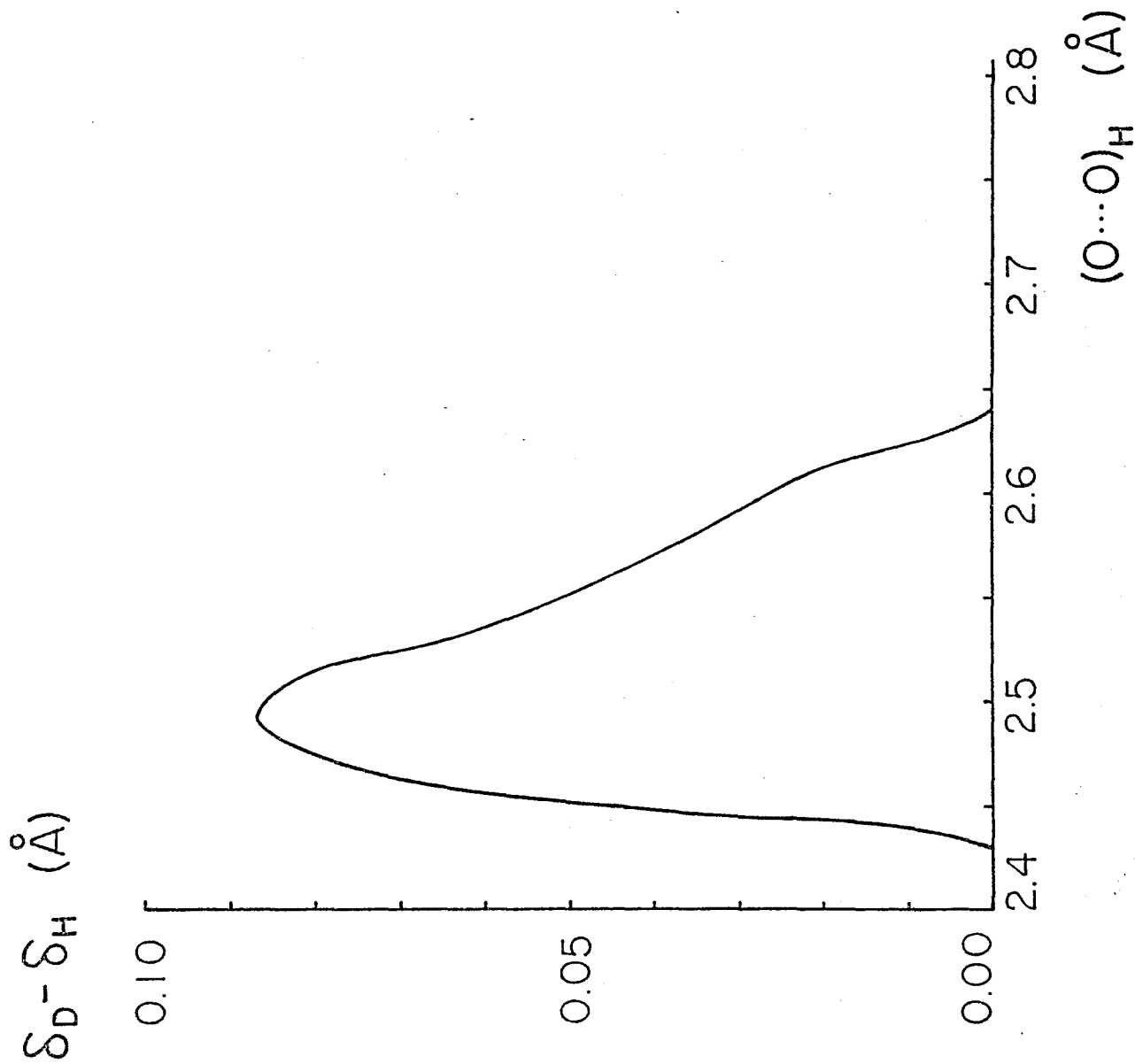
Fig. 5. The isotope effect of the distance between two equilibrium position in a symmetric bond, $\delta_D - \delta_H$, as a function of $(O \cdots O)_H$ length.

length is in a region of $\Delta R > 0$ and is longer than that expected for a single-minimum type bond. The relevant values of some ferro-, antiferroelectric, and other materials are listed in Table 2. The data are compatible with the above statement. ΔT_c is large when the hydrogen bond is symmetric and O...O is in the range of about 2.5-2.6 $\overset{\circ}{A}$. ΔT_c is only about 10° or negative when O...O length is around 2.44 $\overset{\circ}{A}$ even if symmetric, or when the hydrogen bond is asymmetric even if O...O is in a range of 2.5-2.6 $\overset{\circ}{A}$. However, in order to confirm this relation further examination may be necessary both by the structural and by the dielectric studies.

Table 2. O...O distance in the paraelectric phase, Curie temperature T_c and its shift on deuteration ΔT_c in some ferro- and antiferroelectrics

The O...O distance is the room temperature value if not specified. F and AF denote ferro-and antiferroelectric respectively. The references to structural data are marked with an asterisk and dielectric data were quoted from Landolt-Börnstein[39] if not mentioned expressly.

Compound references		O...O (Å)	Type of bond	T_c (°K)	ΔT_c (°K)	
$NH_4H(ClCH_2COO)_2$	31[*],32	2.432(5)	symmetric	120	11	F
TGS at 330°K	33[*]	2.443(7)	symmetric	322	11	F
KH_2PO_4	25[*]	2.496(1)	symmetric	123	90	F
$NH_4H_2PO_4$	34[*]	2.490(1)	symmetric	148	94	AF
$NH_4H_2AsO_4$	34[*]	2.512(2)	symmetric	216	88	AF
$NaH_3(SeO_3)_2$	14[*]	2.556(6)	asymmetric	194	75	F
		2.602(9)	symmetric			
$RbHSO_4$	35[*],36	2.53 (1)	asymmetric	264	-11	F
		2.62 (1)	asymmetric			
NH_4HSO_4	37[*],38	2.514(6)	asymmetric	270	- 8	F
		2.598(5)	asymmetric			
$KH_3(SeO_3)_2$	13[*],38	2.566(1)	symmetric	201	70	

References

1) K. Nakamoto, M. Margoshes and R. E. Rundle:

 J. Amer. Chem. Soc. 77 (1955) 6480.

2) F. F. Iwasaki, H. Iwasaki and Y. Saito: Acta Cryst.

 23 (1967) 64.; G. C. Pimentel and A. L. McClellan:

 Ann. Rev. phys. Chem. 22 (1971) 347.

3) W. C. Hamilton and J. A. Ibers: Hydrogen Bonding in

 Solids (Benjamin, New York, 1968).

4) J. C. Speakman: Structure and Bonding 12 (1972) 141.

5) J. M. Robertson and A. R. Ubbelohde: Proc. Roy.

 Soc. London. A170 (1939) 222; A. R. Ubbelohde:

 Proc. Roy. Soc. London. A173 (1939) 417;

 A. R. Ubbelohde and I. Woodward: Proc. Roy. Soc.

 London. A179 (1942) 399.

6) M. Ichikawa: Acta Cryst. B34 (1978) 2074.

7) I. D. Brown: Acta Cryst. A32 (1976) 24.

8) I. Olovsson and P. -G. Jönsson: The Hydrogen Bond,

 ed. P. Schuster, G. Zundel and C. Sandorfy

 (North-Holland, Amsterdam,1976) Vol.II, chap.8.

9) T. Yamamoto, M. Negishi, M. Ushimaru, Y. Tozawa,

 K. Okabe and S. Fujiwara: Proc. 2nd USA-Japan

 Computer Conf. (1975) 159.

10) UNICS Universal Crystallographic Computing System,

 ed. T. Sakurai (Crystallographic Society of Japan,

 1967).

11) H. N. Shrivastava and J. C. Speakman: J. chem Soc.

 (1961) 1151.

12) A. Sequeira, C. A. Berkebile and W. C. Hamilton:
J. mol. Struct. $\underset{\sim}{1}$ (1967) 283; Å. Nilsson, R. Liminga
and I. Olovsson: Acta Chem. Scand. $\underset{\sim}{22}$ (1968) 719;
M. Currie and J. C. Speakman: J. Chem. Soc. A.
(1970) 1923; B. Dickens, E. Prince, L. W. Schroeder
and W. E. Brown: Acta Cryst. B$\underset{\sim}{29}$ (1973) 2057.

13) M. S. Lehmann and F. K. Larsen: Acta Chem. Scand.
$\underset{\sim}{25}$ (1971) 3859.

14) S. F. Kaplan, M. I. Kay and B. Morosin:
Ferroelectrics $\underset{\sim}{1}$ (1970) 31.

15) A. Novak: Structure and Bonding $\underset{\sim}{18}$ (1974) 177.

16) R. G. Delaplane and J. A. Ibers: Acta Cryst.
B$\underset{\sim}{25}$ (1969) 2423 ; T. M. Sabine, G. W. Cox,
B. M. Craven: Acta Cryst. B$\underset{\sim}{25}$ (1969) 2437;
P. Coppens and T. M. Sabine: Acta Cryst. B$\underset{\sim}{25}$
(1969) 2442.

17) R. E. Rundle: J. Phys. Radium $\underset{\sim}{25}$ (1964) 487.

18) T. R. Singh and J. L. Wood: J. chem. Phys.
$\underset{\sim}{50}$ (1969) 3572.

19) J. E. Finholt and J. M. Williams: J. chem. Phys.
$\underset{\sim}{59}$ (1973) 5114.

20) J. O. Thomas: Acta Cryst. B$\underset{\sim}{28}$ (1972) 2037.

21) M. Catti and G. Ferraris: Acta Cryst. B$\underset{\sim}{32}$ (1976) 2754.

22) M. Tokunaga: Ferroelectrics $\underset{\sim}{1}$ (1970) 195;
G. A. Samara: Ferroelectrics $\underset{\sim}{5}$ (1973) 25.

23) D. Semmingsen: Acta Chem. Scand. $\underset{\sim}{27}$ (1973) 3961;
ibid A$\underset{\sim}{29}$ (1975) 470.

24) G. D. Brunton and C. K. Johnson: J. chem Phys.
    62 (1975) 3797.

25) J. Nakano, Y. Shiozaki and E. Nakamura: J. Phys. Soc.
    Japan 34 (1973) 1423.

26) J. O. Thomas, R. Tellgren and I. Olovsson:
    Acta Cryst. B30 (1974) 1155; ibid B30 (1974) 2540.

27) J. O. Thomas: Acta Cryst. B29 (1973) 1767.

28) T. Kjällman and I. Olovsson: Acta Cryst. B28 (1972)
    1692.

29) R. Tellgren and I. Olovsson: J. chem. Phys.
    54 (1971) 127.

30) A. L. Macdonald, J. C. Speakman and D. Hadži:
    J. Chem Soc. Perkin II. (1972) 825.

31) M. Ichikawa: Acta Cryst. B28 (1972) 755.

32) H. Chihara, A. Inaba, N. Nakamura and T. Yamamoto:
    J. Phys. Soc. Japan 35 (1973) 1480.

33) K. Itoh and T. Mitsui: Ferroelectrics 5 (1973) 235.

34) A. A. Khan and W. H. Baur: Acta Cryst.
    B29 (1973) 2721.

35) J. P. Ashmore and H. E. Petch: Can. J. Phys.
    53 (1975) 2694.

36) M. Kasahara and I. Tatsuzaki: J. Phys. Soc. Japan
    38 (1975) 1389.; M. Kasahara: private communication.

37) R. J. Nelmes; Acta Cryst. B27 (1971) 272.

38) E. C. Subbarao; Ferroelectrics 5 (1973) 267.

39) T. Mitsui: Landolt-Börnstein. Numerical Data and
    Functional Relationships in Science and Technology

ed. K. -H. Hellwege and A. M. Hellwege

(Springer, Berlin, 1969) New Series III/3.

Ferro- and Antiferroelectrice Substances

Chapter V. Summary

The X-ray crystal structure analyses of ferroelectric

$NH_4H(ClCH_2COO)_2$ have been carried out both in the paraelectric

phase at room temperature and in the ferroelectric phase

at 80K. The refinements of a block-diagonal least-squares

method resulted in the final R value of 0.068 for the counter

data (0.070 for the photographic data) with anisotropic

temperature factors at room temperature and in the final R

value of 0.106 for the photographic data with isotropic

temperature factors at 80K.

It has been found that $NH_4H(ClCH_2COO)_2$ has the shortest

symmetric hydrogen bond connecting two chloroacetate residues,

2.432 $\overset{\circ}{A}$ at room temperature among hydrogen-bonded ferroelectrics

precisely measured so far. It has been concluded that the

shape of the H-atom potential is effectively of a single-

minimum type and $NH_4H(ClCH_2COO)_2$ offers the first example

with a single-minimum potential well, judging from the O...O length

and the anomalies in the infrared spectrum together with a

complete agreement of the combined consideration of neutron

diffraction and spectroscopic data, and so on in other Type

A acid salts.

This result necessarily led to the conclusion that the

acidic hydrogen atom does not play the crucial role in the phase

transition, (not the trigger) in contrast to the hydrogen atom in a double-minimum potential well, on the basis of which ordinarily the phase transitions in hydrogen-bonded ferroelectrics such as KH_2PO_4 are considered. The above conclusion was supported by the results of the structure analysis at 80K, which showed no definite change in the conformation of the chloroacetate dimer including a very short hydrogen bond of 2.457(16)$\overset{o}{A}$ as compared with the room-temperature structure, whereas a considerable shift was observed in the ammonium ion. It has been shown that there is no contradiction between the conclusion drawn from our present structure analyses and those from other experimental technique mainly by Chihara and coworkers, i.e. the ^{35}Cl nuclear quadrupole resonance frequency and relaxation time, the heat capacity measurement, and infrared and Raman spectra.

A possibility of a pure order-disorder mechanism of the nitrogen atom of the ammonium ion was examined, but ruled out by the comparison of the observed and calculated shape of contours in Fourier maps and the r.m.s amplitude of thermal vibrations. This conclusion is also compatible with the ^{35}Cl spin-spin relaxation time and the proton magnetic resonance measurements.

The correlation between O-H vs O...O distances and the geometric isotope effect in OHO bonds have been investigated on the basis of recent accurate X-ray and

neutron crystal-structure data. Symmetric bonds are continuously distributed at least to about 2.6 $\overset{\circ}{A}$, in which the shape of the H atom potential curve seems to vary continuously from single to double-minimum type with increasing O...O diatance, retaining the symmetry requirement. The average correlation curve of asymmetric bonds appears to coincide with 'symmetric' straight line at the shortest limit around 2.4 $\overset{\circ}{A}$. On deuteration an expansion was seen in the O...O distance range 2.44-2.64 $\overset{\circ}{A}$, with a maximum value of 0.027 $\overset{\circ}{A}$.

The equilibrium position of the H atom in symmetric bonds was considered with the correlation curve of O-H vs O...O distance and the geometric isotope effect used as empirical basis, under the assumption that the potential curve can be expressed as the superposition of two asymmetric bonds. The correspondence was pointed out between two kinds of isotope effect, i.e. the isotope effect of the distance between two equilibrium positions or the geometric isotope effect and the isotope effect of the transition temperature of hydrogen-bonded crysrals which undergo ferro-, antiferroelectric, and other structural phase transitions; The shift of the transition temperature is large when the hydrogen bond is symmetric and O...O is in a range of 2.5-2.6 $\overset{\circ}{A}$.

Appendix

Table.   Hydrogen-bond parameters as determined by
neutron diffraction

Only OHO bonds are included, and these only if the bond
lengths have standard deviations equal to or less than
0.010 $\overset{\circ}{A}$, the O...O distance is less than 3 $\overset{\circ}{A}$, and the
O-H...O angle is larger than 150°.   Numbers in parentheses
are the standard deviations in the least significant digit.
All distances are uncorrected for thermal motion.

Compound and reference	O...O (Å)	O–H (Å)	H...O (Å)	O–H...O (degrees)	Comments
MnCl$_2$·4H$_2$O El Saffar AC B27, 66 (1971) *	2.923(2)	0.963(2)	1.969(3)	170.4(2)	
	2.964(2)	0.953(3)	2.014(3)	174.4(3)	
Th(NO$_3$)$_4$·5H$_2$O Taylor AC 20, 842 (1966)	2.697(4)	0.971(5)	1.726(5)	177.5(6)	
	2.698(4)	0.953(6)	1.749(6)	173.2(5)	
	2.901(4)	0.954(6)	1.962(6)	167.9(6)	
	2.953(4)	0.961(6)	1.996(5)	173.6(6)	
UO$_2$(NO$_3$)$_2$·2H$_2$O Dalley IC 10, 323 (1971)	2.834(3)	0.961(5)	1.892(5)	166.1(5)	
	2.924(4)	0.961(5)	1.964(5)	179.8(6)	
	2.899(4)	0.951(4)	1.982(5)	161.2(4)	
Ba(ClO$_3$)$_2$·H$_2$O Sikka JCP 48, 1883 (1968)	2.891(5)	0.926(10)	1.991(10)	163.6(9)	
BeSO$_4$·4H$_2$O Sikka AC B25, 310 (1969)	2.617(5)	0.967(6)	1.656(8)	171.7(8)	
	2.684(5)	0.971(8)	1.719(6)	172.3(6)	
MgSO$_4$·7H$_2$O Ferraris JCSDT 816 (1973)	2.692(6)	0.967(7)	1.726(7)	176.4(7)	
	2.703(7)	0.976(9)	1.732(9)	172.8(7)	
	2.728(5)	0.961(7)	1.772(7)	173.1(6)	
	2.734(5)	0.985(8)	1.758(9)	170.9(7)	
	2.704(7)	0.956(9)	1.758(9)	169.7(7)	
	2.756(6)	0.959(10)	1.804(10)	172.1(7)	
	2.768(7)	0.963(9)	1.810(9)	172.9(8)	
	2.792(6)	0.957(9)	1.842(9)	172.0(8)	
	2.825(6)	0.975(8)	1.854(8)	173.9(6)	
	2.820(7)	0.962(10)	1.891(9)	161.7(8)	
	2.901(6)	0.952(9)	1.961(8)	169.6(8)	
	2.923(6)	0.972(8)	1.965(8)	168.0(6)	
	2.903(6)	0.959(10)	1.980(10)	161.0(9)	

Compound and reference	O...O (Å)	O–H (Å)	H...O (Å)	O–H...O (degrees)	Comments
Cu(NH$_4$)$_2$(SO$_4$)$_2$·6H$_2$O Brown AC B25, 676 (1969)	2.683(2)	0.976(3)	1.715(3)	171.3(2)	
	2.707(2)	0.978(3)	1.730(3)	178.1(3)	
	2.732(2)	0.981(3)	1.760(3)	170.4(3)	
	2.743(2)	0.978(3)	1.765(3)	177.5(3)	
	2.826(2)	0.964(3)	1.871(3)	170.1(3)	
	2.821(2)	0.963(3)	1.871(3)	168.7(3)	
CaHPO$_4$·2H$_2$O Curry JCSA 3725 (1971)	2.781(6)	0.971(9)	1.811(8)	175.7(11)	
	2.831(7)	0.944(10)	1.902(10)	167.3(14)	
KH$_5$(PO$_4$)$_2$ Phillippot RCM 9, 825 (1972)	2.422(3)	1.174(4)	1.252(4)	173.0(3)	
	2.567(3)	0.994(5)	1.574(5)	176.6(4)	
	2.592(3)	1.009(5)	1.583(4)	177.5(3)	
	2.579(3)	0.994(5)	1.586(4)	176.6(3)	
	2.624(3)	0.991(5)	1.638(5)	173.4(3)	
Ca(H$_2$AsO$_4$)$_2$ Ferraris AC B28, 2430 (1972)	2.436(3)	1.218(1)	1.218(1)	180.0(0)	symmetric ($\bar{1}$)
	2.444(3)	1.222(1)	1.222(1)	180.0(0)	symmetric ($\bar{1}$)
	2.659(2)	1.001(3)	1.663(3)	173.9(3)	
	2.692(2)	0.994(3)	1.725(3)	163.4(3)	
	2.875(2)	0.966(3)	1.997(3)	150.2(3)	
CaHAsO$_4$·H$_2$O Ferraris AC B28, 209 (1972)	2.632(6)	0.998(10)	1.657(10)	164.6(8)	
InOOH Lehmann ACS 24, 1662 (1970)	2.537(3)	1.079(7)	1.458(7)	179.1(6)	
Te(OH)$_6$ Lindqvist ACS 27, 85 (1973)	2.685(2)	0.990(3)	1.698(3)	174.5(2)	
	2.676(2)	0.987(3)	1.704(3)	167.2(3)	
	2.695(2)	0.989(3)	1.711(3)	173.4(3)	
	2.696(2)	0.977(3)	1.720(3)	175.8(3)	
	2.709(2)	0.983(3)	1.727(3)	175.3(3)	
	2.730(2)	0.983(3)	1.750(3)	175.1(3)	

Compound and reference	O...O (Å)	O–H (Å)	H...O (Å)	O–H...O (degrees)	Comments
H₂SeO₃ Larsen ACS 25, 1233 (1971)	2.621(2) 2.667(2)	1.009(3) 0.986(3)	1.621(3) 1.749(3)	170.6(3) 153.4(3)	
LiH₃(SeO₃)₂ Tellgren JSSC 4, 255 (1972)	2.518(3) 2.552(3) 2.646(4)	1.141(7) 1.040(6) 1.003(4)	1.378(7) 1.517(6) 1.649(5)	176.6(5) 173.3(4) 172.3(4)	
KH₃(SeO₃)₂ Lehmann ACS 25, 3859 (1971)	2.566(1) 2.602(2)	1.044(7) 1.029(3)	1.529(6) 1.575(3)	171.1(4) 175.2(2)	symmetric (2)
LiHCOO.H₂O Tellgren F 6, 191 (1974)	2.714(2) 2.896(2)	0.976(3) 0.965(4)	1.742(3) 1.949(4)	173.6(3) 166.6(3)	
KHC₂O₄ Moore INCL 7, 873 (1971)	2.518(3)	1.054(5)	1.467(5)	174.6(4)	
K₂C₂O₄.H₂O Sequeira AC B26, 77 (1970)	2.754(2)	0.963(3)	1.801(3)	169.7(2)	
(COOH)₂.2H₂O α-form Sabine AC B25, 2437 (1969)	2.506(4) 2.864(5) 2.881(4)	1.026(7) 0.964(7) 0.956(9)	1.480(7) 1.917(8) 1.979(9)	179.3(6) 166.9(6) 156.6(7)	
CH₃COOH.H₃PO₄ Jönsson ACS 26, 1599 (1972)	2.558(4) 2.574(3) 2.590(3) 2.594(3) 2.617(4) 2.667(4) 2.681(4) 2.688(4)	1.005(6) 1.009(6) 0.995(5) 0.987(5) 0.962(6) 0.985(6) 0.986(7) 0.992(8)	1.558(5) 1.570(5) 1.596(5) 1.609(5) 1.662(5) 1.685(5) 1.697(6) 1.699(6)	172.9(4) 172.3(4) 176.7(4) 175.5(5) 171.1(5) 174.2(4) 175.4(4) 175.2(5)	

Compound and reference	O...O (Å)	O–H (Å)	H...O (Å)	O–H...O (degrees)	Comments
HOCH₂COOH Ellison AC B27, 333 (1971)	2.638(2) 2.647(2) 2.714(2) 2.696(2)	1.001(2) 1.003(2) 0.971(3) 0.970(3)	1.640(2) 1.646(2) 1.753(3) 1.774(3)	175.2(2) 175.5(3) 169.7(2) 157.6(2)	
KH oxydiacetate Albertsson AC B29, 2751 (1973)	2.476(2)	1.152(3)	1.328(3)	174.2(3)	
RbH oxydiacetate Albertsson AC B29, 2751 (1973)	2.449(3)	1.226(2)	1.226(2)	175.0(4)	symmetric (2)
KH bis(trifluoroacetate) Macdonald JCSPTII 825 (1972)	2.437(4)	1.218(2)	1.218(2)	180.0(0)	symmetric ($\bar{1}$)
KH diaspirinate Sequeira JMS 1, 283 (1968)	2.448(4)	1.224(2)	1.224(2)	180.0(0)	symmetric ($\bar{1}$)
KH malonate Currie JCSA 1923 (1970)	2.468(6)	1.234(3)	1.234(3)	180.0(0)	symmetric ($\bar{1}$)
KH chloromaleate Ellison AC 19, 260 (1965)	2.403(3)	1.199(5)	1.206(5)	175.4(4)	intramolecular
KH succinate McAdam JCSA 1994 (1971)	2.444(9)	1.227(6)	1.227(6)	169.3(9)	symmetric (2)
$H_3O^+CH_3C_6H_4SO_3^-$ Lundgren JCP 58, 788 (1973)	2.520(5) 2.525(5) 2.538(5)	1.013(8) 1.011(8) 1.008(8)	1.508(7) 1.516(7) 1.535(7)	178.0(5) 174.3(5) 172.3(5)	
$H_5O_2^+C_6H_2(NO_2)_3SO_3^- \cdot 2H_2O$ Lundgren AC B30, 1937 (1974)	2.436(2) 2.604(3) 2.621(2) 2.685(2) 2.734(2)	1.128(4) 0.996(4) 0.988(3) 0.977(4) 0.976(4)	1.310(4) 1.609(4) 1.634(3) 1.720(4) 1.776(3)	175.0(3) 177.2(3) 176.4(3) 168.7(3) 166.4(3)	

Compound and reference	O...O (Å)	O–H (Å)	H...O (Å)	O–H...O (degrees)	Comments
Dialuric acid·H₂O Craven AC B25, 1970 (1969)	2.571(7)	1.007(8)	1.574(9)	169.8(7)	
D-Glucitol A-form Park AC B27, 2393 (1971)	2.652(5)	0.986(7)	1.695(7)	162.5(7)	
	2.676(5)	0.966(8)	1.724(8)	168.2(6)	
	2.669(5)	0.953(8)	1.730(8)	168.0(8)	
	2.882(6)	0.980(9)	1.915(9)	168.3(8)	
	2.991(6)	0.972(9)	2.019(9)	177.9(7)	
(NH₄)₂C₂O₄·H₂O Taylor AC B28, 3340 (1972)	2.773(3)	0.982(5)	1.807(5)	166.8(5)	
Sucrose Brown AC B29, 790 (1973)	2.716(2)	0.976(3)	1.760(3)	165.4(3)	
	2.781(2)	0.974(3)	1.851(3)	158.6(3)	
	2.855(2)	0.972(3)	1.892(3)	170.2(3)	intramolecular
	2.850(2)	0.972(3)	1.895(3)	167.1(3)	intramolecular
	2.862(2)	0.959(3)	1.907(3)	172.8(3)	
	2.864(2)	0.969(3)	1.908(3)	168.5(2)	
	2.848(2)	0.956(4)	1.921(4)	162.9(3)	
NH₄HC₂O₄·H₂C₂O₄·2H₂O Currie JCSA 1862 (1967)	2.500(4)	1.102(7)	1.399(7)	177.1(7)	
	2.472(4)	1.069(7)	1.403(9)	178.2(6)	
	2.520(5)	1.040(7)	1.483(10)	173.3(7)	
	2.721(4)	0.966(7)	1.765(7)	169.5(6)	
	2.745(4)	0.973(6)	1.787(6)	167.4(6)	
	2.833(5)	0.949(8)	1.906(7)	164.8(7)	
	2.899(5)	0.945(8)	2.000(8)	158.2(7)	
N₂H₅H₂PO₄ Jönsson ACS 25, 1729 (1971)	2.517(7)	1.072(10)	1.446(10)	176.9(9)	
	2.561(7)	1.023(10)	1.542(10)	173.9(10)	

Compound and reference	O...O (Å)	O-H (Å)	H...O (Å)	O-H...O (degrees)	Comments
$N_2H_6(H_2PO_4)_2$ Kvick ACS 26, 1087 (1972)	2.609(2) 2.643(2)	0.995(4) 1.003(3)	1.616(4) 1.643(3)	175.3(4) 174.7(3)	
$N_2H_5HC_2O_4$ Nilsson ACS 22, 719 (1968)	2.448(7)	1.224(4)	1.224(4)	180.0(0)	symmetric ($\bar{1}$)
$(NH_2)_2CO.H_3PO_4$ Kostansek AC B28, 2454 (1972)	2.421(3) 2.589(3) 2.658(3)	1.207(6) 0.999(4) 0.997(5)	1.223(6) 1.591(4) 1.664(5)	169.9(4) 176.4(4) 173.7(4)	
$(NH_2)_2COH^+NO_3^-$ Worsham AC B25, 572 (1969)	2.596(2)	1.006(3)	1.591(3)	178.2(3)	
$[Ni(C_5H_{11}N_2O)_2H^+]Cl^-.H_2O$ Schlemper JCP 54, 3990 (1971)	2.420(5)	1.187(5)	1.242(5)	169.9(4)	intramolecular
L-Asparagine.H_2O Verbist AC B28, 3006 (1972)	2.812(2) 2.843(2)	0.957(3) 0.962(3)	1.879(3) 1.888(3)	164.3(3) 171.5(3)	
L-Glutamic acid β-form Lehmann JCMS 2, 225 (1972)	2.519(2)	1.050(4)	1.475(5)	172.3(3)	
L-Lysine.HCl.$2H_2O$ Koetzle AC B28, 3207 (1972)	2.805(5)	0.960(9)	1.857(7)	169.2(7)	
Glycylglycine.HCl.H_2O Koetzle AC B28, 2083 (1972)	2.644(5) 2.728(4)	1.003(7) 0.972(6)	1.658(6) 1.764(6)	166.8(5) 170.7(6)	
DL-Serine Frey AC B29, 876 (1973)	2.671(1)	0.981(1)	1.692(2)	175.1(1)	

Compound and reference	O...O (Å)	O–H (Å)	H...O (Å)	O–H...O (degrees)	Comments
L-Serine.H_2O Frey AC B29, 876 (1973)	2.785(4) 2.809(5) 2.877(5)	0.958(7) 0.946(7) 0.955(8)	1.843(6) 1.868(6) 1.922(7)	166.8(4) 173.2(5) 177.4(5)	
L-Arginine.$2H_2O$ Lehmann JCSPTII 133 (1973)	2.738(4) 2.715(5)	0.974(6) 0.946(7)	1.770(6) 1.789(7)	172.1(5) 164.9(7)	
L-Tyrosine Frey JCP 58, 2547 (1973)	2.666(3)	0.981(4)	1.689(4)	173.8(3)	
L-Tyrosine.HCl Frey JCP 58, 2547 (1973)	2.619(4)	1.018(6)	1.609(5)	170.7(4)	
4-Hydroxy-L-proline Koetzle AC B29, 231 (1973)	2.792(2)	0.971(3)	1.843(3)	164.9(3)	
$Cu_2(CH_3COO)_4 \cdot 2H_2O$ Brown AC B29, 2393 (1973)	2.823(2) 2.927(2)	0.961(3) 0.949(3)	1.863(3) 1.994(3)	179.2(3) 167.1(3)	
$LiClO_4 \cdot 3H_2O$ Sequeira AC B31, 1735 (1975)	2.989(2)	0.972(7)	2.044(7)	163.6(8)	
$HgSO_4 \cdot 4H_2O$ Baur AC 17, 863 (1964)	2.884(5) 2.833(6) 2.734(5)	0.969(10) 0.989(10) 0.981(10)	1.919(10) 1.847(10) 1.753(10)	173.6(8) 173.8(9) 177.7(9)	
$NaCO_3 \cdot H_2O$ Wu AC B31, 890 (1975)	2.677(7) 2.905(6)	0.988(9) 0.967(10)	1.699(8) 1.987(9)	169.9(8) 157.9(8)	

Compound and reference	O...O (Å)	O – H (Å)	H...O (Å)	O-H...O (degrees)	Comments
$K_2[Cu(H_2O)_6](SO_4)_2$ Robinson CSC 1, 185 (1972)	2.742(4)	0.977(6)	1.775(6)	170.4(5)	
	2.781(5)	0.974(6)	1.813(7)	171.9(5)	
	2.711(4)	0.978(5)	1.733(6)	178.0(5)	
	2.764(5)	0.960(6)	1.805(6)	176.1(5)	
	2.668(4)	0.976(6)	1.697(6)	173.3(5)	
	2.657(5)	0.983(6)	1.680(6)	171.7(4)	
$Rb_2[Cu(H_2O)_6](SO_4)_2$ vanderZee CSC 1, 367 (1972)	2.741(8)	0.971(5)	1.772(7)	175.0(5)	
	2.754(9)	0.970(7)	1.791(8)	171.8(5)	
	2.688(7)	0.971(6)	1.724(7)	171.7(5)	
$Cs_2[Cu(H_2O)_6](SO_4)_2$ Shields CSC 1, 189 (1972)	2.714(7)	1.019(10)	1.704(9)	170.9(7)	
	2.780(7)	0.986(10)	1.798(9)	173.2(8)	
	2.702(7)	1.014(10)	1.697(9)	170.5(6)	
$Tl_2[Cu(H_2O)_6](SO_4)_2$ Shields CSC 1, 371 (1972)	2.730(7)	0.985(8)	1.751(8)	172.1(6)	
	2.758(7)	0.978(8)	1.787(9)	171.6(6)	
	2.753(7)	0.999(7)	1.756(7)	175.1(7)	
	2.707(7)	0.986(7)	1.728(8)	171.6(6)	
K D-Gluconate.H_2O A-form Panagiotopoulos AC B30, 1421 (1974)	2.726(5)	0.956(7)	1.783(6)	168.1(5)	
	2.776(4)	0.963(6)	1.834(6)	165.3(5)	
	2.938(4)	0.946(6)	2.001(6)	171.0(5)	
	2.639(4)	0.973(5)	1.666(5)	177.3(5)	
	2.872(4)	0.977(6)	1.982(6)	150.4(5)	
B-form	2.745(5)	0.965(7)	1.805(7)	164.2(6)	
	2.784(5)	0.966(7)	1.817(7)	178.0(6)	
	2.844(5)	0.961(7)	1.887(7)	173.2(6)	
	2.894(5)	0.963(7)	1.974(7)	159.1(6)	
	2.783(5)	0.975(7)	1.809(7)	178.0(6)	
	2.885(5)	0.972(7)	1.915(7)	176.2(6)	
α-Resorcinol Bacon ZK 138, S.19 (1973)	2.717(4)	0.985(6)	1.734(5)	175.9(5)	
	2.732(5)	0.987(7)	1.765(7)	165.7(5)	

Compound and reference	O...O (Å)	O-H (Å)	H...O (Å)	O-H...O (degrees)	Comments
(H₃PO₄)₂·H₂O Dickens AC B30, 1470 (1974)	2.563(1) 2.581(1) 2.580(1) 2.611(1) 2.659(1) 2.692(2)	1.008(2) 1.011(2) 1.002(2) 1.001(2) 0.989(2) 0.985(3)	1.556(2) 1.571(2) 1.583(2) 1.618(2) 1.675(2) 1.714(2)	176.2(2) 176.6(2) 171.8(2) 170.3(2) 172.2(2) 171.5(2)	
LiH₂PO₃ Johansson AC B32, 412 (1976)	2.558(4)	1.018(4)	1.547(4)	171.6(3)	
Ca(H₂PO₄)₂ Dickens AC B29, 2057 (1973)	2.620(4) 2.677(5) 2.817(4) 2.434(5) 2.419(6)	1.000(8) 1.000(8) 0.957(8) 1.218(3) 1.210(3)	1.625(7) 1.710(6) 1.922(8) 1.218(3) 1.210(3)	173.6(6) 162.8(6) 154.5(6) 180.0(0) 180.0(0)	 symmetric (1̄) symmetric (1̄)
Ca(H₂PO₄)₂·H₂O Schroeder AC B31, 9 (1975)	2.595(3) 2.622(3) 2.694(3) 2.626(3)	1.016(4) 0.987(5) 0.983(5) 0.987(5)	1.584(4) 1.679(4) 1.728(5) 1.653(5)	172.5(3) 172.3(4) 166.4(5) 167.5(4)	
NH₄H₃(SeO₃)₂ Tellgren AC B30, 2497 (1974)	2.644(4) 2.596(4) 2.554(4)	1.007(5) 1.004(7) 1.027(5)	1.643(5) 1.595(6) 1.532(6)	172.3(5) 174.3(5) 172.4(5)	
YH(C₂O₄)₂·3H₂O Brunton JCP 62, 3797 (1975)	2.440(3) 2.643(2) 2.680(2)	1.221(1) 0.983(3) 0.992(3)	1.221(1) 1.674(3) 1.688(3)	175.3(3) 167.9(3) 178.2(3)	symmetric (2)
KHCO₃ Thomas AC B30, 2540 (1974)	2.587(1)	1.005(2)	1.587(2)	173.0(2)	
CCl₃CH(OH)₂ Brown CSC 2, 107 (1973)	2.903(2) 2.838(2)	0.975(2) 0.972(2)	1.929(2) 1.915(2)	176.7(2) 157.5(2)	

Compound and reference	O...O (Å)	O - H (Å)	H...O (Å)	O-H...O (degrees)	Comments
K₂[Cu(H₂O)₆](SeO₄)₂ Whitnall CSC 4, 709 (1975)	2.868(3)	0.958(4)	1.924(4)	167.8(4)	
	2.821(3)	0.969(5)	1.867(5)	167.7(4)	
	2.655(3)	0.976(3)	1.679(3)	178.8(4)	
	2.718(3)	1.001(4)	1.719(3)	175.4(4)	
	2.677(4)	0.980(5)	1.700(4)	174.5(3)	
	2.654(3)	1.003(4)	1.657(4)	171.6(3)	
K₂[Cu(H₂O)₆](SO₄)₂ Hodgeson CSC 4, 713 (1975)	2.784(3)	0.980(3)	1.813(3)	170.5(4)	
	2.795(3)	0.965(5)	1.838(4)	170.8(3)	
	2.658(2)	0.975(3)	1.684(4)	178.2(4)	
	2.737(3)	0.987(4)	1.755(4)	173.1(4)	
	2.715(3)	0.959(4)	1.766(4)	169.3(3)	
	2.656(3)	0.985(4)	1.681(4)	170.1(3)	
K₂[Zn(H₂O)₆](SO₄)₂ Whitnall CSC 4, 717 (1975)	2.679(6)	0.976(9)	1.703(8)	179.3(7)	
	2.746(6)	1.002(10)	1.746(9)	175.1(8)	
	2.726(6)	1.000(10)	1.734(10)	170.7(7)	
	2.642(7)	0.967(10)	1.684(9)	170.6(6)	
[Zn(H₂O)₄[Hg(CN)₂]₂][NO₃]₂·3H₂O Power JCSDT 2072 (1975)	2.728(3)	0.952(6)	1.777(5)	176.3(4)	
	2.724(4)	0.976(5)	1.750(5)	175.7(4)	
	2.753(4)	0.995(4)	1.769(5)	169.4(4)	
	2.756(5)	0.968(5)	1.792(6)	173.6(4)	
	2.861(4)	0.976(5)	1.887(6)	175.7(5)	
Quinolinic acid Kvick JCP 60, 3866 (1974)	2.398(3)	1.163(5)	1.238(5)	174.4(4)	intramolecular
Squaric acid Wang JCSPTII 35 (1974)	2.544(4)	1.028(7)	1.516(7)	178.8(9)	
	2.532(4)	1.104(9)	1.435(9)	171.8(9)	
Methyl α-D-Altropyranoside Poppleton AC B31, 2400 (1975)	2.879(4)	0.961(6)	1.922(6)	173.0(6)	
	2.702(4)	0.971(5)	1.737(5)	172.8(5)	
Tetraacetylethane Power JCMS 5, 59 (1975)	2.450(4)	1.194(9)	1.319(9)	154.3(4)	intramolecular
3,3'-Trithiobis-(2,4-pentanedione) Power JCMS 5, 125 (1975)	2.457(4)	1.141(7)	1.388(8)	152.6(5)	intramolecular

* only first author's name is quoted and journal names are abbreviated as follows :

AC	Acta Cryst.	JCSA	J. Chem. Soc. (A)
ACS	Acta Chem. Scand.	JCSDT	J. Chem. Soc. Dalton Trans.
CSC	Cryst. Struct. Commun.	JCSPTII	J. Chem. Soc. Perkin Trans. II
F	Ferroelectrics	JMS	J. Mol. Struct.
IC	Inorg. Chem.	JSSC	J. Solid State Chem.
INCL	Inorg. Nucl. Chem. Letters	RCM	Rev. Chim. Mineral.
JCMS	J. Cryst. Mol. Struct.	ZK	Z. Kristallogr.
JCP	J. Chem. Phys.		

Acknowledgements

    The author wishes to express his deep gratitude to
his thesis advisor, Professor Hideaki Chihara for critical
reading the thesis, invaluable discussions and suggestions
in the course of the studies of ferroelectric $NH_4H(ClCH_2COO)_2$.

    He also wishes to thank Professor emeritus Hiroshi
Mizutani and Professor Takashi Watanabe of Hokkaido University
for their understanding and encouragement of this research.

    He is very grateful to his colleagues and many staffs
of Department of Physics, Hokkaido University for their
helpful advise and cooperation.